cirrhosis. Rats were divided into 5 groups consisting of 15 or 10 rats each. In groups 1–4, the diet contents were the same as those in experiment A. Group 5 (CSAA plus JTE-522 at 30 mg · $kg^{-1}$ · $day^{-1}$) was set to examine the potential toxicity of JTE-522. Experiment C was designed to examine the effects of delayed administration of JTE-522. Thus, groups 1 and 2 received CDAA alone during the initial 12 weeks and then CDAA plus JTE-522 at a low or high dose for the subsequent 24 weeks (12–36 weeks).

TAA-induced liver fibrosis model. Control groups (n = 5) were given chow diet for 6 weeks. Liver fibrosis was produced by repeated intraperitoneal injections of TAA (200 mg/kg; Wako Pure Chemical Industries, Osaka, Japan) 3 times per week for 6 weeks (n = 8).[20] In another group, 8 rats that received TAA injection were fed chow diet plus JTE-522 at 15 mg · $kg^{-1}$ · $day^{-1}$ for 6 weeks.

The rats in each group were killed under light ether anesthesia at the end of each experiment. The livers and other organs were immediately dissected out and examined macroscopically. For histopathologic and immunohistochemical examinations, tissue samples were fixed in 10% neutral buffered formalin, processed through graded ethanol solutions, and embedded in paraffin. A portion of the liver samples was immediately frozen in liquid nitrogen and stored at −80°C. Serum was collected from blood samples and stored at −80°C.

### Reagents

Anti-murine COX-2 polyclonal antibody and the blocking peptide that was used to generate COX-2 antibody, the COX-2 electrophoresis standard, were obtained from Cayman Chemical (Ann Arbor, MI).[21] Anti-rat glutathione *S*-transferase placental form (GST-P) polyclonal antibody was obtained from Medical & Biological Laboratories Co. (Nagoya, Japan).[22] Anti-human α–smooth muscle actin (α-SMA) monoclonal antibody (clone 1A4), which cross-reacts with rat α-SMA but not mouse α-SMA, was obtained from Dako (Carpinteria, CA).[23] Anti-rat CD45 (also designated as leukocyte common antigen) monoclonal antibody was obtained from PharMingen (San Diego, CA).[24] Anti-human actin polyclonal antibody, which cross-reacts with rat actin, was obtained from Sigma Chemical Co. (St. Louis, MO). Anti-human monoclonal proliferating cell nuclear antigen (PCNA) antibody, which cross-reacts with rat PCNA, was purchased from Novocastra Laboratories (Benton Lane, Newcastle, England).[25]

### Collagen Staining

Collagen staining was performed using a collagen staining kit (Collagen Research Center, Tokyo, Japan) according to the method described by the supplier.[26] Briefly, paraffin-embedded liver sections were prepared in 4-μm thickness, deparaffinized in xylene, and rehydrated. After washing twice with phosphate-buffered saline for 10 minutes each, the slides were incubated for 1 hour at room temperature with staining solution A, which specifically reacts with collagen. The slides were then washed 3 times with phosphate-buffered saline and once with distilled water for 5 minutes each. The tissue fraction containing collagen is stained in red.

### Immunohistochemistry

Immunostaining was performed as described previously by our laboratories.[8,9] Briefly, after deparaffinization, heat antigen retrieval was performed in 10 mmol/L citrate buffer, pH 6.0, at 95°C for 40 minutes. The slides were then processed for immunohistochemistry on the TeckMate Horizon automated staining system (DAKO, Glostrup, Denmark) using the Vectastain ABC-peroxidase kit (Vector Laboratories, Burlingame, CA). In the step of primary antibody reaction, the slides were incubated with the GST-P, COX-2, CD45, and PCNA antibodies (final concentration: 1:500, 1:100, 1:100, and 1:50, respectively) for 1 hour at room temperature. For positive controls, Jurkat cells were used for CD45 staining[24] and human colon cancer tissue was used for COX-2 staining.[9] Normal crypts in the colon of rats served as a positive control for PCNA staining.[25] The control sections of GST-P–positive minifoci in the early stages of rat hepatocarcinogenesis were kindly provided by Medical & Biological Laboratories Co. The specificity of positive staining with COX-2 antibody was further verified by absorption test using blocking peptide. For negative controls, phosphate-buffered saline was used as a substitute for the primary antibody to exclude false-positive responses from nonspecific binding of immunoglobulin G or from the secondary antibody.

### Evaluation of Histology, Liver Fibrogenesis, and GST-P–Positive Preneoplastic Nodules

The processes of liver fibrosis, cirrhosis, and HCC were assessed by H&E staining (by H.Y. and K.W.). The criteria of Squire and Levitt[27] were used for the diagnosis of rat HCC. A 30-$cm^2$ area, which corresponded to approximately 40–45 slides, was examined in each liver. For assessment of liver fibrogenesis, collagen-stained areas were measured by a computer-assisted image analysis system with Mac Scope software (Mitani Co., Fukui, Japan),[9] and the relative area of fibrosis to the whole liver was calculated. GST-P staining is a reliable marker of preneoplastic lesions in rat hepatocarcinogenesis.[22] The numbers of GST-P–positive preneoplastic nodules were counted under the microscope. The area of GST-P–positive preneoplastic nodules was measured by a computer-assisted image analysis system and expressed as positive area per 1 $cm^2$.

### Evaluation of CD45 and PCNA Staining

For analysis of CD45 or PCNA index, the fields of periportal area or fibrotic septa of each liver sample were surveyed for CD45- or PCNA-positive cells. A 30-$cm^2$ area was examined in each liver, and positive cell number/$cm^2$ was calculated.

### Western Blot Analysis

Approximately 50 mg of liver sample was homogenized in 0.5 mL of RIPA buffer (25 mmol/L Tris, pH 7.4, 50 mmol/L NaCl, 0.5% sodium deoxycholate, 2% Nonidet P-40, and 0.2% sodium dodecyl sulfate) containing protease inhibitors (1 mmol/L phenylmethylsulfonyl fluoride, 10 μg/mL aprotinin, and 10 μg/mL leupeptin). The homogenate was centrifuged at 14,000 rpm for 20 minutes at 4°C. The resulting supernatant was collected, and total protein concentration was determined using the Bradford protein assay (Bio-Rad, Hercules, CA). Western blot analysis was performed as described in our previous studies.[28,29] Briefly, 100 μg of the total protein was premixed with loading buffer (0.05 mol/L Tris-HCl [pH 6.8], 2% sodium dodecyl sulfate, 0.2 mol/L β-mercaptoethanol, 10% glycerol, and 0.001% bromophenol blue), boiled for 5 minutes, and subjected to sodium dodecyl sulfate/polyacrylamide protein gel electrophoresis on 10% gel. After electrophoresis, protein transfer was performed onto a polyvinylidene difluoride membrane using a transblot apparatus in a buffer containing 0.02 mol/L Tris-HCl (pH 8.3), 0.2 mol/L glycine, and 20% methanol. After blocking in 10% skim milk, the membrane was incubated with the primary antibody, anti–COX-2 (1:100 dilution), anti–α-SMA (1:200 dilution), or anti-actin (1:1000 dilution) for 1 hour at room temperature. After 3 washes each for 5 minutes with Tris-buffered saline (0.02 mol/L Tris-HCl [pH 7.5] and 0.1 mol/L NaCl) containing 0.2% Tween 20, the filter was incubated with the secondary antibody at a dilution of 1:2000. The protein bands were detected using the Amersham enhanced chemiluminescence detection system (Amersham, Arlington Heights, IL) according to the instructions provided by the manufacturer. For positive controls, the purified COX-2 protein (Cayman Chemical) and human cirrhotic liver tissues that cross-react with the currently used anti–α-SMA antibody[23] were used. An absorption test was performed to verify the specificity of the COX-2 antibody.

### Measurement of $PGE_2$ Levels

To measure basal $PGE_2$ levels in the liver, approximately 50-mg frozen liver samples were homogenized on ice in 0.5 mL of 0.1 mol/L Tris-HCl buffer and vortexed thoroughly for 3 minutes. $PGE_2$ levels in supernatants were determined using an enzyme immunoassay kit for $PGE_2$ (Cayman Chemical) and a UV detector (Wako Pure Chemical Industries) using the instructions provided by the manufacturer.[17]

### Biochemical Assay of Aspartate Aminotransferase

Aspartate aminotransferase activities in the serum samples were enzymatically analyzed using a selective chemistry analyzer (Arkray, Osaka, Japan).

### Quantitative Real-Time Polymerase Chain Reaction

The frozen tissue specimens were crashed in TRIzol reagent (Life Technologies, Vienna, Austria). RNA extraction was performed according to the instructions provided by the supplier. Purified RNA was quantified and assessed for purity by UV spectrophotometry. Complementary DNA was generated from 1 μg RNA with avian myeloblastosis virus reverse transcriptase using the Reverse Transcription System (Promega, Madison, WI) according to the instructions provided by the supplier. Quantitative polymerase chain reaction (PCR) was performed using Light Cycler (Roche Diagnostics, Mannheim, Germany) as described previously.[9] The PCR primers used for detection of c-myc and β-actin were prepared as reported previously.[30,31] Briefly, 20 μL of PCR reaction components, with Light Cycler/Fast Start DNA Master SYBRGreen I (Roche Diagnostics), contained 0.25 μmol/L of each primer, 2 μmol/L $MgCl_2$, and 2 μL complementary DNA as a template. PCR conditions were set up as follows: one cycle of denaturing at 95°C for 2 minutes, followed by 40 cycles of 95°C for 15 seconds, 62°C for 10 seconds, and 72°C for 40 seconds. Fluorescence was acquired at the end of every 72°C extension phase. Quantification data from each sample were analyzed using Light Cycler analysis software. In this analysis, the background fluorescence was subtracted by setting a noise band. The concentration of the target was obtained by plotting against a standard curve. Rat IEC18 intestinal cell line was used as the standard (i.e., use of known concentrations). The amount of c-myc was normalized by that of β-actin. For verifying the specific product, we analyzed the melting temperature curves of final PCR products.

### Statistical Analysis

Statistical analysis was performed using the Statview J-5.0 program (Abacus Concepts, Inc., Berkeley, CA). For multiple comparisons, the Dunnett method was used together with least squares means to provide appropriate correction. Differences between 2 groups were analyzed by Student $t$ test. $P < 0.05$ indicated a statistically significant difference.

## Results

### CDAA Model

Food intake. The amount of food intake of each type of diet was estimated every week up to 36 weeks and per rat for each group in experiment B, and no significant differences were found among the groups with regard to the consumed amount of different diets (CDAA and CSAA, with or without JTE-522, data not shown).

Results of experiment A (12 weeks). *Histopathologic changes.* Rats fed CDAA exclusively had several prominent histopathologic changes in the liver at 12 weeks, such as accumulation of free fatty acid in hepatocytes, increase in the number of fibrous septa, and loss of structure of hepatic lobules (Figure 1*A*). Addition of

**Table 2.** Results of Experiment A

| Groups | No. of rats | Final body weight (g)[a] | Fibrosis ($cm^2/cm^2$)[a] | GST-P–positive lesions[a] No./$cm^2$ | GST-P–positive lesions[a] Area ($mm^2/cm^2$) |
|---|---|---|---|---|---|
| Experiment A | | | | | |
| CDAA alone | 5 | 321 ± 3.0 | 0.132 ± 0.009 | 4.1 ± 0.5 | 0.22 ± 0.04 |
| CDAA + JTE-522 (10 mg · $kg^{-1}$ · $day^{-1}$) | 5 | 338 ± 4.9[b] | 0.041 ± 0.002[c] | 1.7 ± 0.2[d] | 0.07 ± 0.03[c] |
| CDAA + JTE-522 (30 mg · $kg^{-1}$ · kg · $day^{-1}$) | 5 | 345 ± 4.8[d,e] | 0.007 ± 0.002[f,g] | 0[c,g] | 0[c,g] |
| CSAA alone | 5 | 346 ± 2.5[f] | 0.006 ± 0.001[f] | 0[f] | 0[f] |

[a]Values are means ±SD.
[b]NS compared with group 1.
[c]$P < 0.01$, compared with group 1.
[d]$P < 0.05$, compared with group 1.
[e]$P < 0.01$, compared with group 2.
[f]$P < 0.001$, compared with group 1.
[g]$P < 0.001$, compared with group 2.

JTE-522 to CDAA inhibited these changes, and such inhibition was more evident at a higher dose than at a lower dose. Thus, the use of a low dose (10 mg · $kg^{-1}$ · $day^{-1}$) of JTE-522 resulted in reduction of fat accumulation and mild fibrosis (Figure 1*B*); at 30 mg · $kg^{-1}$ · $day^{-1}$, JTE-522 resulted in marked inhibition of fat accumulation and fibrogenesis with preservation of the hepatic architecture (Figure 1*C*). Figure 1*D* shows the histology of normal liver of rats fed the control CSAA.

*Body weight, fibrosis, and GST-P–positive lesions.* Table 2 summarizes the changes in body weight, extent of liver fibrosis, and number and area of GST-P–positive preneoplastic nodules. At 12 weeks, CDAA caused a decrease in body weight, which is a finding consistent with those of other reports.[18,19] CDAA caused extensive fibrosis, as detected by collagen staining (Figure 2*A*), and the appearance of GST-P–positive lesions (Figure 2*B*) in the livers compared with CSAA (Table 2). CSAA produced no GST-P–positive lesions at 12 weeks. Low-dose JTE-522 plus CDAA inhibited fibrogenesis and formation of GST-P–positive nodules. Furthermore, high-dose JTE-522 plus CDAA completely inhibited these changes and resulted in body weight similar to the CSAA-treated control group, only minimal fibrosis, and no GST-P–positive nodules.

**Results of experiment B (36 weeks).** The gross appearances of representative livers in groups 1–4 of experiment B are shown in Figure 3. CDAA alone resulted in the development of fatty cirrhotic liver in all rats (Figure 3*A*), whereas other groups of rats did not show any gross changes (Figure 3*B–D*). Histopathologic examination showed that CDAA induced liver cirrhosis in 15 of 15 rats (100%) and HCC in 13 of 15 rats (87%) (Table 3 and Figure 4*A*). In contrast, no cirrhotic nodules or HCCs were noted in the other diet treatment groups. Rats fed CDAA and treated with low-dose JTE-522 showed only fatty changes and fibrogenesis in the liver (Figure 4*B*). However, rats fed CDAA and treated with high-dose JTE-522 showed only mild fatty changes and mild fibrogenesis (Figure 4*C*). No histopathologic changes were noted in the livers of the CSAA-alone group (Figure 4*D*). It was found that CDAA-treated groups exclusively showed marked infiltration of mononuclear cells into the fibrous tissues within the liver (Figure 4*A*), whereas JTE-522–treated groups showed only occasional infiltration.

**Table 3.** Incidence of Cirrhosis and HCC in Experiments B and C

| Groups | Cirrhosis No. of rats | Cirrhosis Incidence (%) | HCC Incidence (%) | HCC No./$cm^2$ | HCC Area ($mm^2/cm^2$) |
|---|---|---|---|---|---|
| Experiment B | | | | | |
| CDAA alone | 15 | 15 (100) | 13 (87) | 3.1 ± 0.9 | 0.43 ± 0.11 |
| CDAA + JTE-522 (10 mg · $kg^{-1}$ · $day^{-1}$) | 10 | 0 (0) | 0 (0) | 0 | 0 |
| CDAA + JTE-522 (30 mg · $kg^{-1}$ · $day^{-1}$) | 10 | 0 (0) | 0 (0) | 0 | 0 |
| CSAA alone | 10 | 0 (0) | 0 (0) | 0 | 0 |
| CSAA + JTE-522 (30 mg · $kg^{-1}$ · $day^{-1}$) | 10 | 0 (0) | 0 (0) | 0 | 0 |
| Experiment C | | | | | |
| CDAA + JTE-522 (10 mg · $kg^{-1}$ · $day^{-1}$) | 10 | 0 (0) | 0 (0) | 0 | 0 |
| CDAA + JTE-522 (30 mg · $kg^{-1}$ · $day^{-1}$) | 10 | 0 (0) | 0 (0) | 0 | 0 |

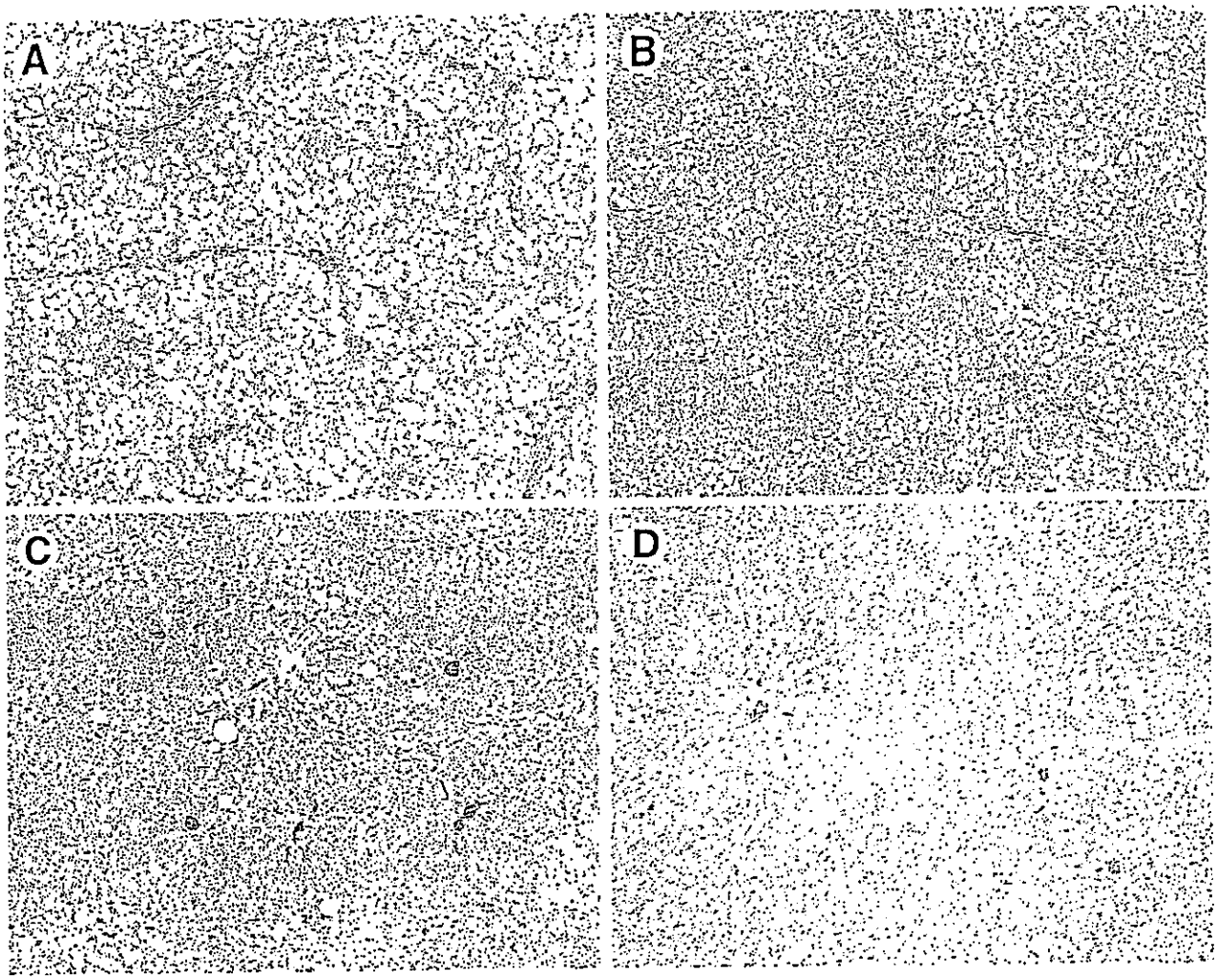


**Figure 1.** Histopathologic findings in livers of representative rats from each group in experiment A (12 weeks). Sections were stained with H&E. (*A*) CDAA caused marked fatty changes and fibrosis. CDAA plus JTE-522 at (*B*) 10 mg · $kg^{-1}$ · $day^{-1}$ and (*C*) 30 mg · $kg^{-1}$ · $day^{-1}$ inhibited histopathologic changes in a dose-dependent manner. (*D*) The liver of a representative rat fed control CSAA. (Original magnification: *A–D*, 100×.)

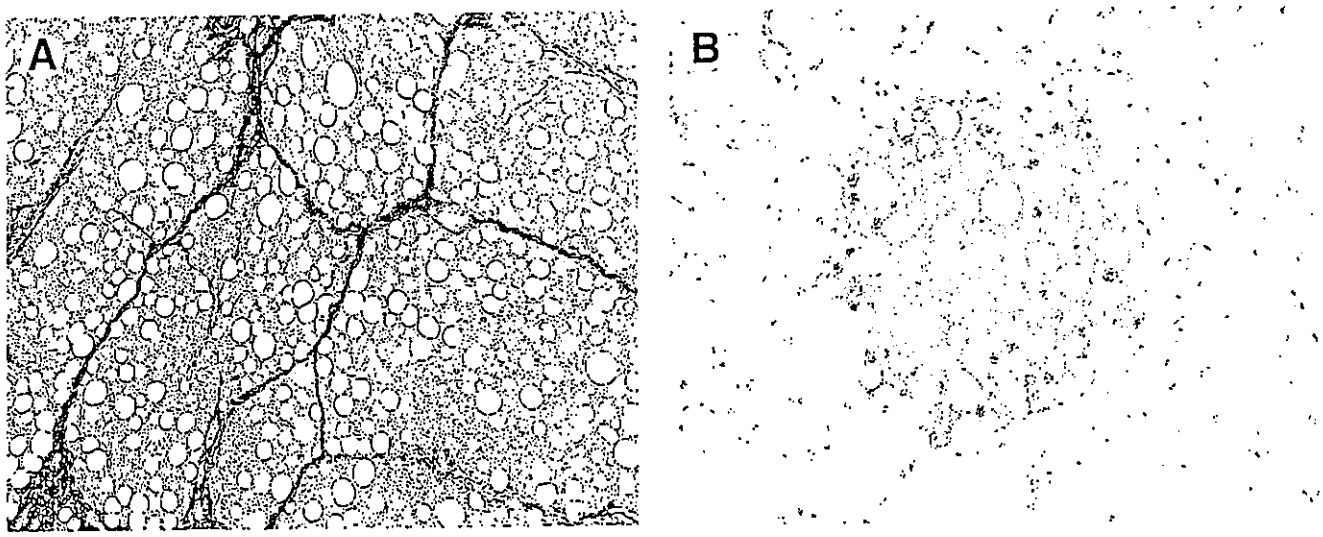


**Figure 2.** (*A*) Collagen staining and (*B*) staining of GST-P–positive preneoplastic nodule. (*A*) Collagen fibers are stained in red. (*B*) Representative GST-P–positive preneoplastic nodule in the liver of rats fed CDAA for 12 weeks. The control sections of GST-P–positive minifoci provided by Medical & Biological Laboratories Co. gave a similar staining pattern (data not shown). (Original magnification: *A*, 200×; *B*, 400×.)

Changes in body weight, fibrosis, and formation of GST-P–positive lesions in experiments B and C are shown in Figure 5. The values in experiment B were essentially an extension of those of experiment A. With CDAA treatment, the amount of fibrous tissue and the number of GST-P–positive nodules increased approximately 3 times and doubled, respectively, compared with those at 12 weeks. The area of GST-P–positive nodules was slightly increased. On the other hand, JTE-522 significantly inhibited CDAA-induced changes in a dose-dependent manner.

*Toxicity of JTE-522.* Group 5 in experiment B was set to monitor the toxicity of JTE-522. The body weights of rats fed CSAA alone or CSAA plus 30 mg · $kg^{-1}$ · $day^{-1}$ JTE-522 for 36 weeks were similar (Figure 5). Group 5 did not show any gross or histopathologic changes in the liver, kidneys, stomach (such as ulcer formation or hemorrhage), pancreas, bladder, intestine, brain, heart, or lungs (data not shown), suggesting that JTE-522 did not cause any apparent toxicity.

**Results of experiment C.** Administration of JTE-522 for 24 weeks had a lesser effect on inhibition of CDAA-induced fibrogenesis and formation of preneoplastic foci compared with the corresponding groups in experiment B (groups 2 and 3) that received continuous administration of JTE-522 for 36 weeks (Figure 5). No cirrhosis or HCC was noted in rats in experiment C (Table 3).

**Expression of COX-2 in liver tissues.** The COX-2 antibody yielded a strong band for the purified COX-2 protein, serving as positive control (Figure 6*A*, upper panel). COX-2 expression increased from normal liver to fatty liver with fibrosis to cirrhotic liver. JTE-522 at a high dose did not affect CSAA-associated low COX-2 expression. However, JTE-522 decreased CDAA-associated high COX-2 expression in a dose-dependent manner. For better comparison between the histopathologic changes and COX-2 expression, immunostaining for the COX-2 protein is shown in Figure 6*B*. In normal livers treated with CSAA for 36 weeks, COX-2 expression was undetectable (Fig. 6*B*, *a*). CDAA-induced fatty liver with fibrosis (12 weeks) expressed a moderate level of the COX-2 protein (Fig. 6*B*, *b*). Most cirrhotic livers in rats treated with CDAA for 36 weeks showed marked COX-2 expression, mainly in the perinuclear region and cytoplasm of the hepatocytes. In addition, fibroblast-like cells and mononuclear cells in the fibrous septum also expressed COX-2 (Fig. 6*B*, *c*). In the groups treated with CSAA plus high-dose JTE-522 or CDAA plus high- or low-dose JTE-522 for 36 weeks (Fig. 6*B*, *d–f*), concordant results with Western blot were obtained.

**Assessment of $PGE_2$ levels, aspartate aminotransferase levels, and PCNA expression.** To examine arachidonate metabolism in the CDAA model, $PGE_2$ level in liver tissues was measured. CDAA led to an increase in $PGE_2$ level time dependently compared with CSAA treatment, and JTE-522 inhibited the change in dose- and time-dependent manners (Figure 7*A*). When aspartate aminotransferase levels were examined by using serum samples, similar results were obtained (Figure 7*B*). PCNA expression was noted in the nuclei of hepatocytes (data not shown). PCNA index also exhibited similar results (Figure 7*C*).

**CD45 Index in liver tissues.** CDAA induced CD45-positive inflammatory cells as early as 12 weeks, and few of these cells were noted at 36 weeks of CDAA treatment (Figure 8*A*, *a* and *B*). At 36 weeks, JTE-522 partially inhibited the appearance of such cells when used at a low dose (Figure 8*A*, *b*) and completely inhibited CD45-positive cells at a high dose (Figure 8*A*, *c*).

**Expression of α-SMA in liver tissue.** Because activated hepatic stellate cells play a role in liver fibrogenesis, we investigated whether JTE-522 affected the amount of activated hepatic stellate cells using α-SMA as a marker.[20,32] Western blot analysis indicated that α-SMA expression was increased from normal liver to fibrotic liver to cirrhosis and JTE-522 dose-dependently reduced α-SMA expression in the CDAA group (Figure 9).

**Expression of c-myc messenger RNA.** CDAA treatment for 36 weeks induced significantly higher expression of c-myc messenger RNA than CSAA treatment (Figure 10). Induction of c-myc gene expression was significantly inhibited by high-dose JTE-522 ($P < 0.01$).

**Figure 3.** Macroscopic appearance of the livers of representative rats of experiment B. (*A*) CDAA alone resulted in the development of fatty cirrhotic liver, whereas (*B–D*) other groups did not show any gross changes (*B*, CDAA + JTE-522, 10 mg · $kg^{-1}$ · $day^{-1}$; *C*, CDAA + JTE-522, 30 mg · $kg^{-1}$ · $day^{-1}$; *D*, CSAA).

**Figure 4.** Histopathologic findings in livers of representative rats from each group in experiment B (36 weeks). Sections were stained with H&E. (*A*) CDAA-induced cirrhotic nodule (left) and HCC (right). Note the marked infiltration of mononuclear cells in the fibrous septa. (*B*) CDAA plus JTE-522 at 10 mg · $kg^{-1}$ · $day^{-1}$ resulted in massive fatty change and prominent fibrogenesis. Some inflammatory cells are present in the fibrous tissues (*arrows*). (*C*) CDAA plus JTE-522 at 30 mg · $kg^{-1}$ · $day^{-1}$ resulted in mild fatty changes and mild fibrogenesis. (*D*) Normal liver of a representative control CSAA rat. (Original magnification: *A–D*, 100×.)

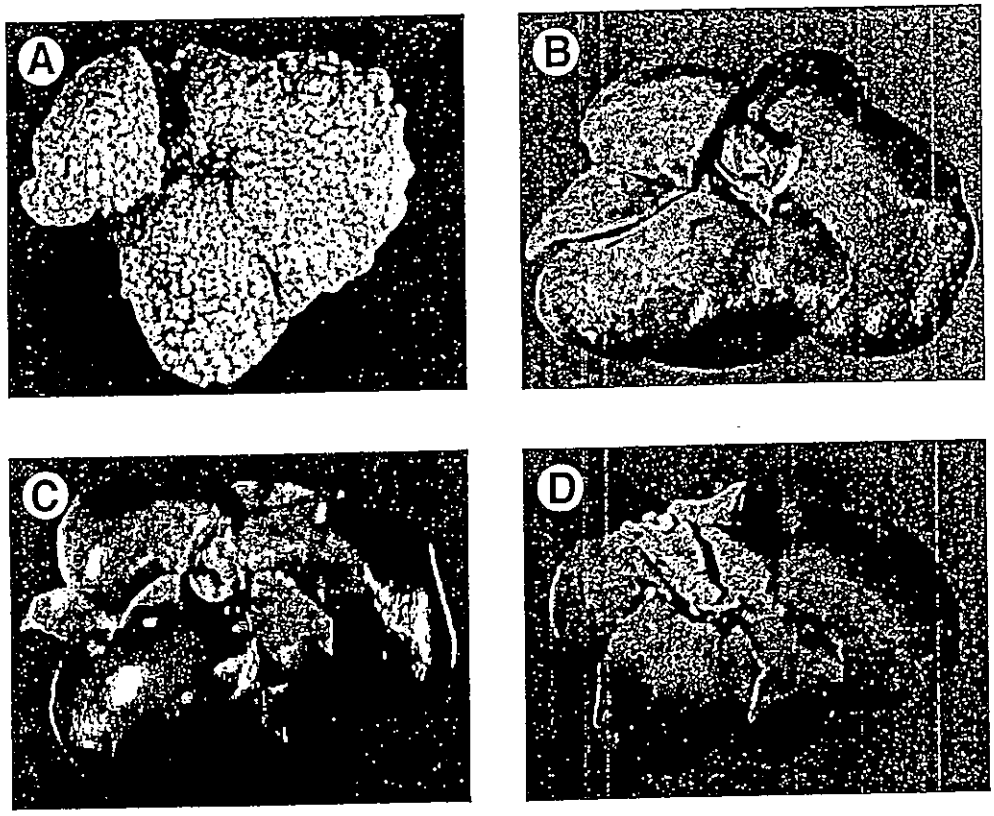


Figure 3.

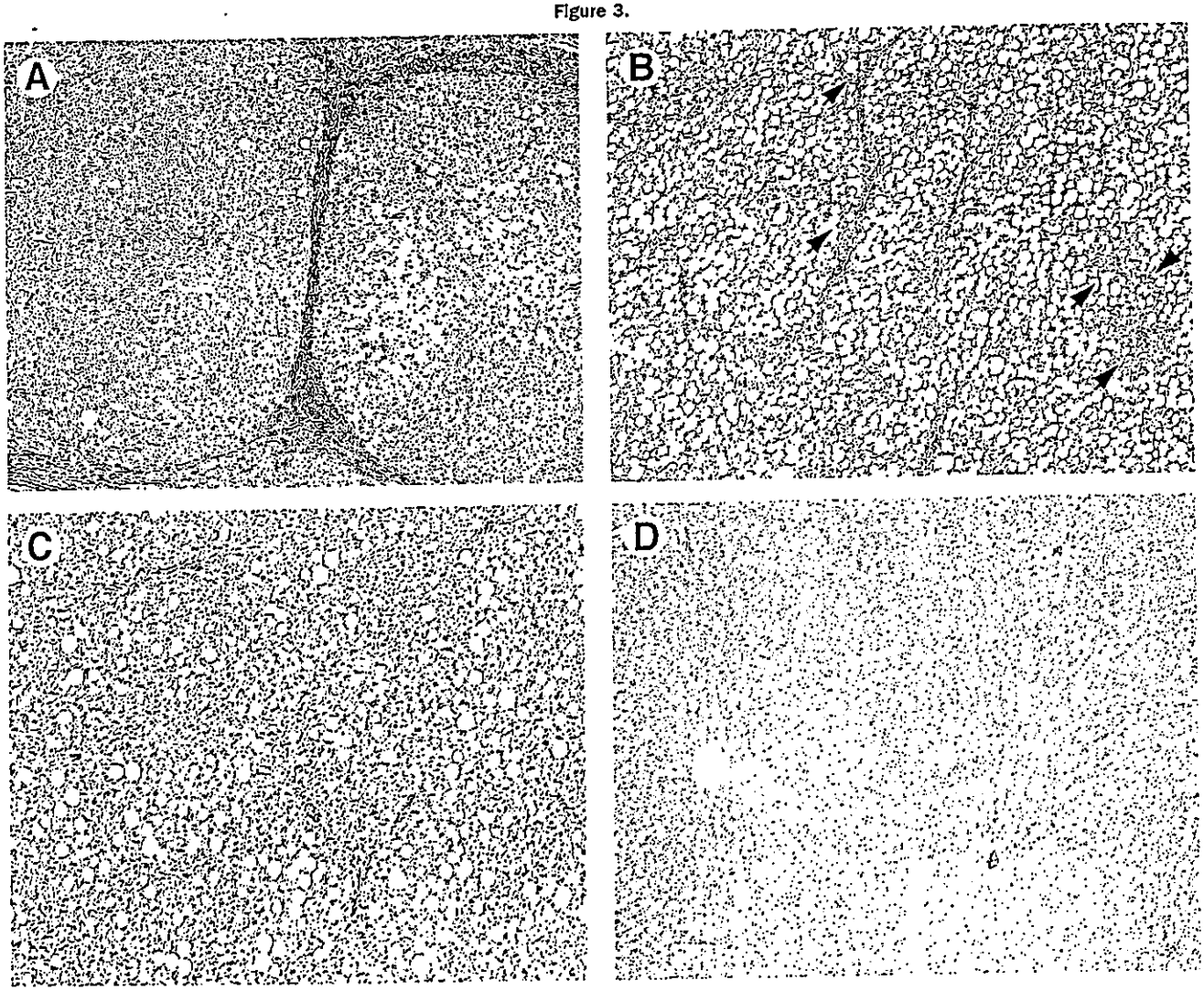


Figure 4.

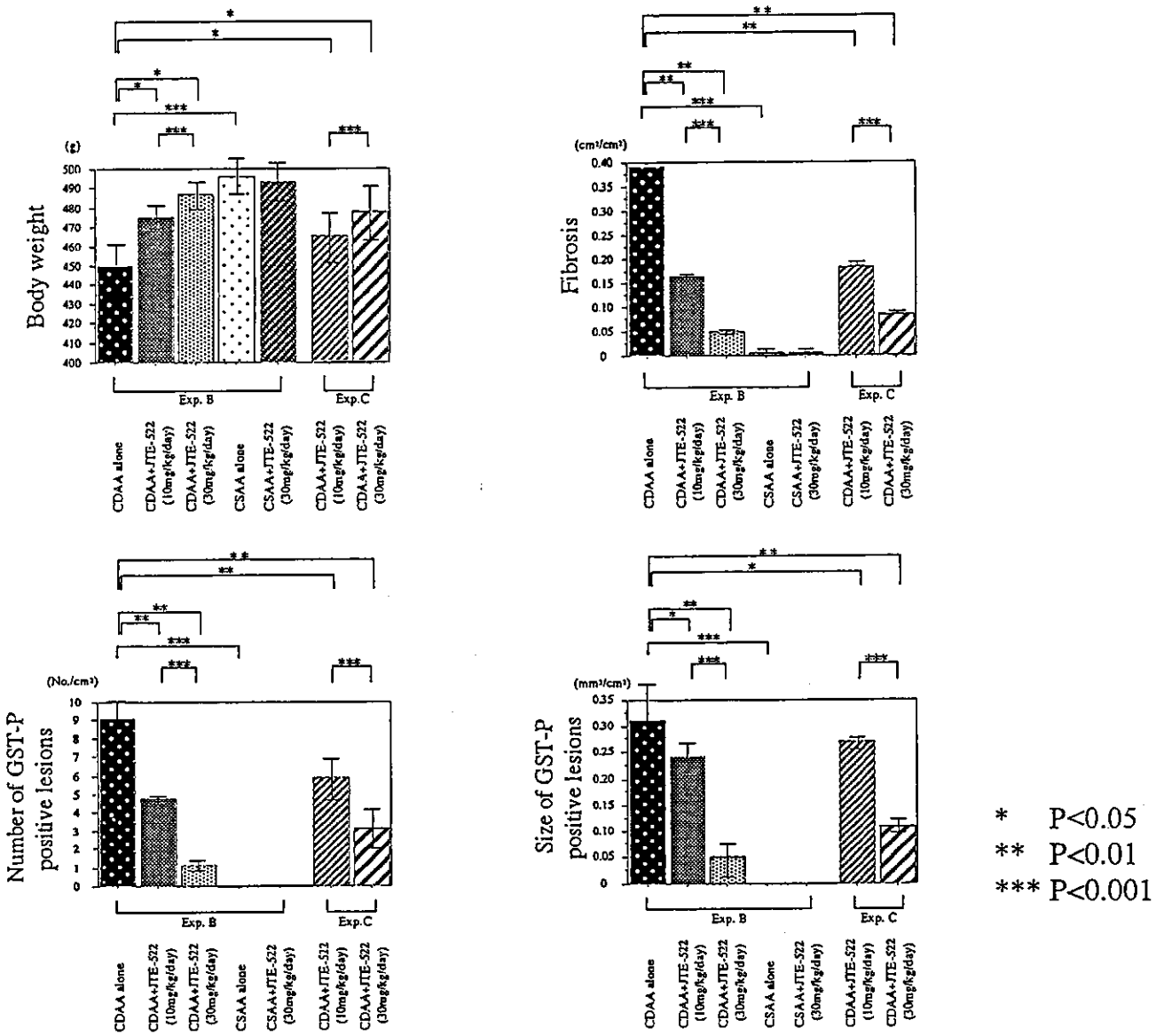


Figure 5. Quantitative analysis of changes in body weight, fibrosis, and GST-P–positive lesions in experiments B and C. Data are mean ± SD.

### TAA-Induced Liver Fibrosis Model

Compared with normal control liver (n = 5), all TAA-treated rats (n = 8) developed marked liver fibrosis with pseudo-lobule formation in the whole liver. TAA-treated rats administered JTE-522 at 15 mg · $kg^{-1}$ · $day^{-1}$ (n = 8) generally showed a weak fibrogenic response in the liver, in which the normal liver architecture was largely well preserved. Collagen staining showed the extent of fibrogenesis in each group (Figure 11*A*), and the difference between the TAA group and the TAA plus JTE-522 group was significant (Figure 11*B*; $P < 0.001$). Western blot analysis showed that α-SMA largely increased in TAA-treated fibrotic livers and administration of JTE-522 reduced α-SMA expression (Figure 11*C*).

## Discussion

Previous studies showed that the nonselective COX inhibitors piroxicam and acetylsalicylic acid prevented cirrhosis and development of preneoplastic nodules in CDAA-treated rats.[18,33] One of the aims of our study was to examine whether selective inhibition of COX-2 alone would be sufficient to realize this goal because such inhibition appears to yield much less toxicity than other nonsteroidal anti-inflammatory drugs. In experiment B, long-term administration of CSAA plus JTE-522 at 30 mg · $kg^{-1}$ · $day^{-1}$ did not induce any toxic side effects, such as body weight loss, gastrointestinal ulceration, bleeding, or renal toxicity, which are

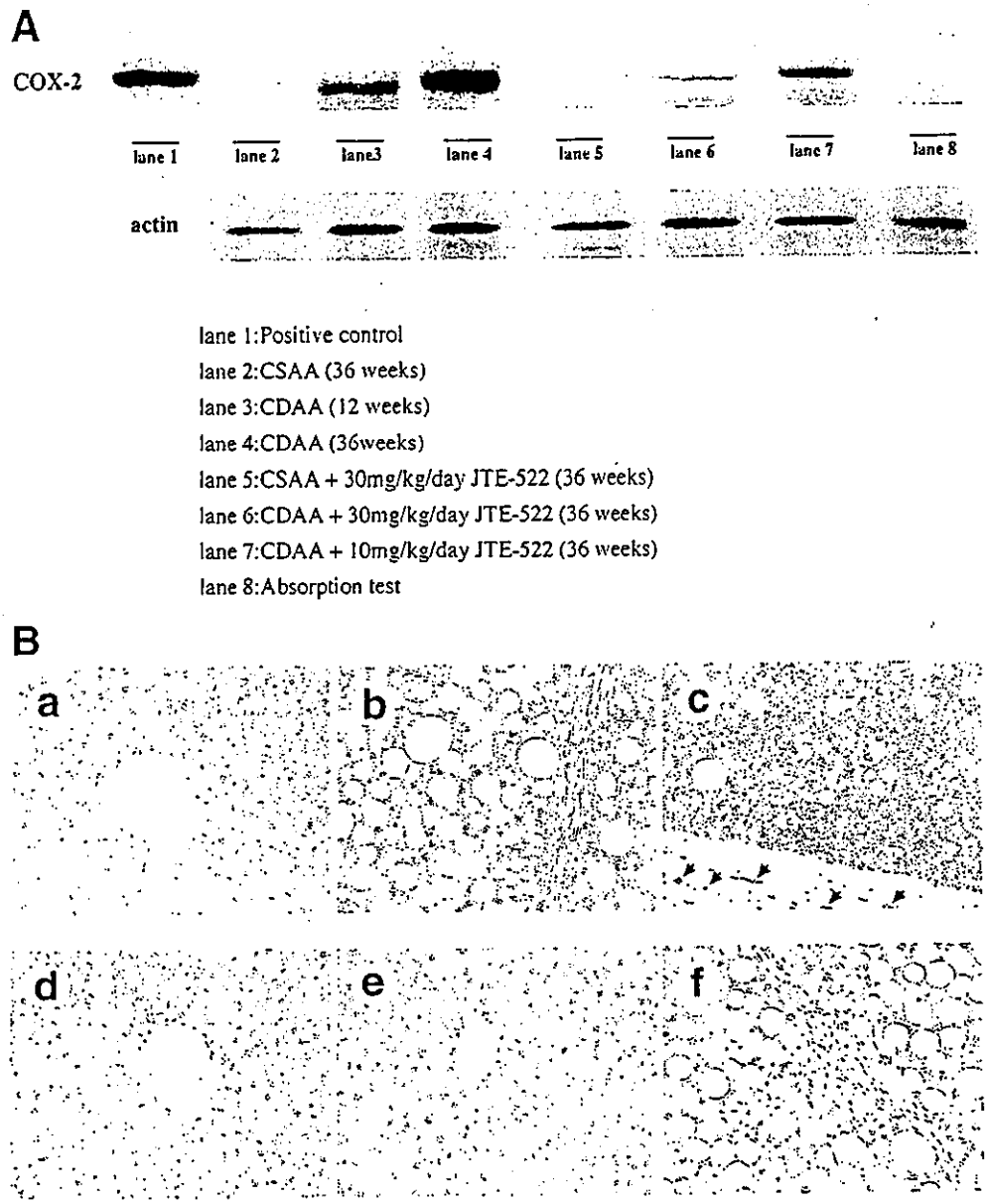


**Figure 6.** COX-2 expression in rat livers. (*A*) Western blot analysis. *Upper panel, lane 1*: positive control of the lysate from a colon cancer tissue; *lane 2*: CSAA (36 weeks); *lane 3*: CDAA (12 weeks); *lane 4*: CDAA (36 weeks); *lane 5*: CSAA containing 30 mg · $kg^{-1}$ · $day^{-1}$ JTE-522 (36 weeks); *lane 6*: CDAA containing 30 mg · $kg^{-1}$ · $day^{-1}$ JTE-522 (36 weeks); *lane 7*: CDAA containing 10 mg · $kg^{-1}$ · $day^{-1}$ JTE-522 (36 weeks); *lane 8*: absorption test. Preabsorbed antibody yielded no band in the lysate from CDAA-treated liver for 36 weeks. *Lower panel*: blots for actin serve as loading controls. (*B*) Immunohistochemistry. (*a*) Normal liver (CSAA, 36 weeks). (*b*) Fibrous liver (CDAA, 12 weeks). (*c*) Cirrhotic liver (CDAA, 36 weeks). Hepatocytes expressed COX-2 protein in the cytoplasm and perinuclear region. Note that mononuclear cells and fibroblast-like cells in fibrous tissues also expressed COX-2 (*arrows*). (*d*) CSAA plus high-dose JTE-522, CDAA plus (*e*) high- or (*f*) low-dose JTE-522 for 36 weeks. (Original magnification 400×.)

major problems caused by nonsteroidal anti-inflammatory drugs.[34] Other investigators also reported that a selective COX-2 inhibitor, SC-236, did not impair renal function in a rat model with liver cirrhosis[35] and that a COX-2 selective inhibitor, celecoxib, did not cause damage of the gastroduodenal mucosa.[36]

CDAA-induced early events include fibrosis, formation of preneoplastic lesions, fatty changes, and loss of hepatic lobule architecture. The results of experiment A (experiments on early events) clearly showed that JTE-522 caused about a 69% and 95% decrease of fibrogenesis when used at low and high doses, respectively (Table 2). The longer experiment B showed a further increase in CDAA-associated fibrogenesis, and the extent of inhibition accomplished by JTE-522 was approximately proportional to that achieved in experiment A. These out-

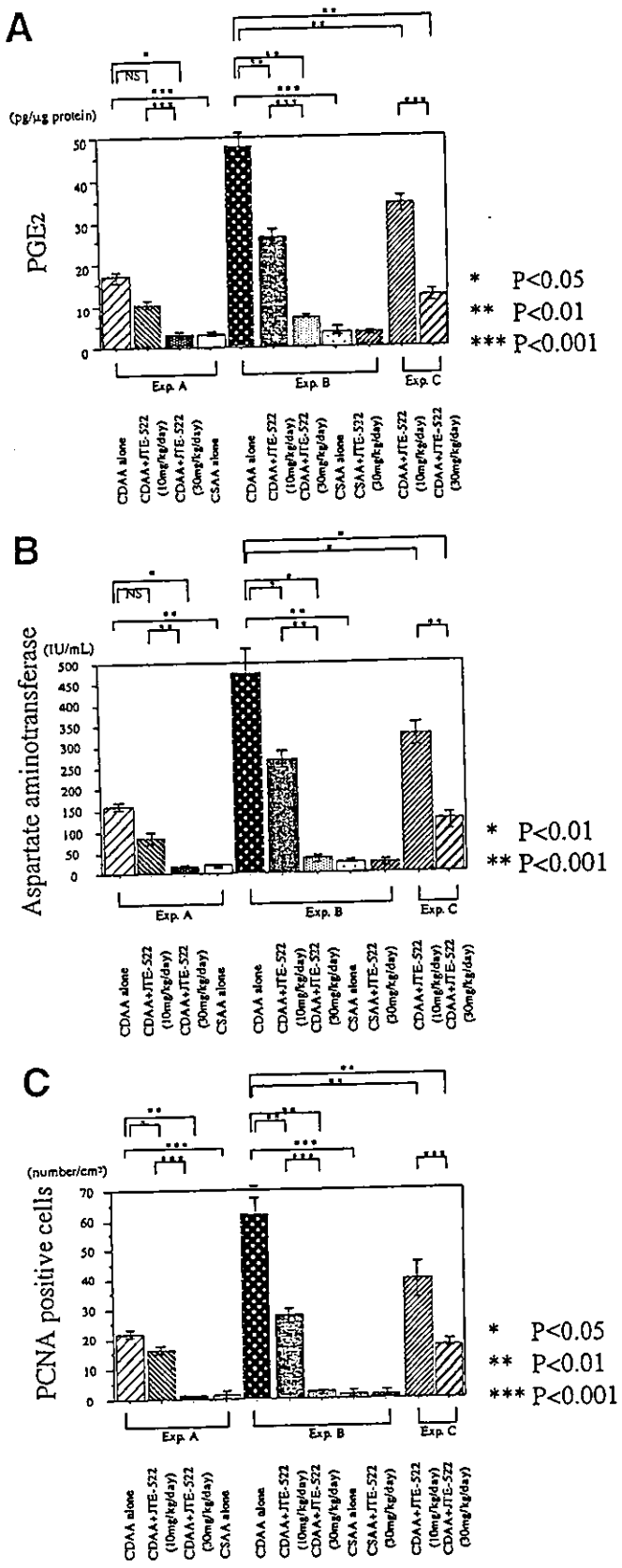


**Figure 7.** (*A*) $PGE_2$ levels, (*B*) serum aspartate aminotransferase levels, and (*C*) PCNA expression in the liver. Each parameter was examined in all rats in experiments A–C. Aspartate aminotransferase level was closely associated with that of $PGE_2$. Data are mean ± SD.

standing results strongly suggest that JTE-522 may be a potent agent against CDAA-induced liver fibrosis. CDAA resulted in the appearance of preneoplastic foci as early as 12 weeks, and development of the lesions was time dependent. The number and area of GST-P–positive foci reflect the potential of initiation and promotion of the preneoplastic lesions, respectively.[22,37] JTE-522 inhibited both processes in a dose-dependent manner.

With regard to the long-term effects of CDAA, high frequencies of cirrhosis and HCC were noted at 36 weeks. Cirrhosis is the final stage of liver fibrosis, and JTE-522 eventually inhibited the development of cirrhosis even when used at a low dose. At the end of experiment B, we were surprised to find that CDAA plus JTE-522–treated rats had normal liver appearance although the livers of most CDAA-treated rats contained multiple small nodules consisting of cirrhotic nodules and HCCs. Detailed microscopic examination confirmed the absence of cirrhotic nodules and HCCs in JTE-522–treated groups. Moreover, even though JTE-522 was administrated from 12 weeks (experiment C), no cirrhosis or HCC were noted at 36 weeks.

Other investigators have also provided sufficient evidence from animal studies indicating that selective COX-2 inhibitors produce effective prevention of carcinogenesis induced by various reagents. However, in these in vivo studies, the suppression rate for cancer formation was only partial even with the highest experimental dose. For example, nimesulide inhibited generation of carcinomas of the bladder, breast, and tongue by 60%, 20%, and 74%, respectively.[38–40] Celecoxib inhibited development of carcinoma of the colon and bladder both by 57%.[41,42] JTE-522 inhibited development of esophageal squamous cell carcinoma by 62%.[17] On the other hand, we found that HCC was very common among CDAA-treated rats (13 of 15; 85%), whereas it was completely inhibited in all CDAA plus JTE-522–treated rats (0 of 10; 0%), that is, an inhibition rate of 100%. Moreover, although JTE-522 exerted a clear dose-dependent inhibition of liver fibrosis and preneoplastic lesions, it did not show dose dependency on cancer formation. These findings may reflect the unique process of hepatocarcinogenesis. Thus, it is probable that establishment of cirrhotic liver may be a prerequisite for further development of HCC in the CDAA model. We postulate that inhibition of fibrogenesis by JTE-522 prevented the development of cirrhosis with effective protection against hepatocarcinogenesis. Because livers showed early changes associated with fibrosis and preneoplastic lesions during the long experiments, even in JTE-522–treated groups, we cannot exclude the possible development of HCC with

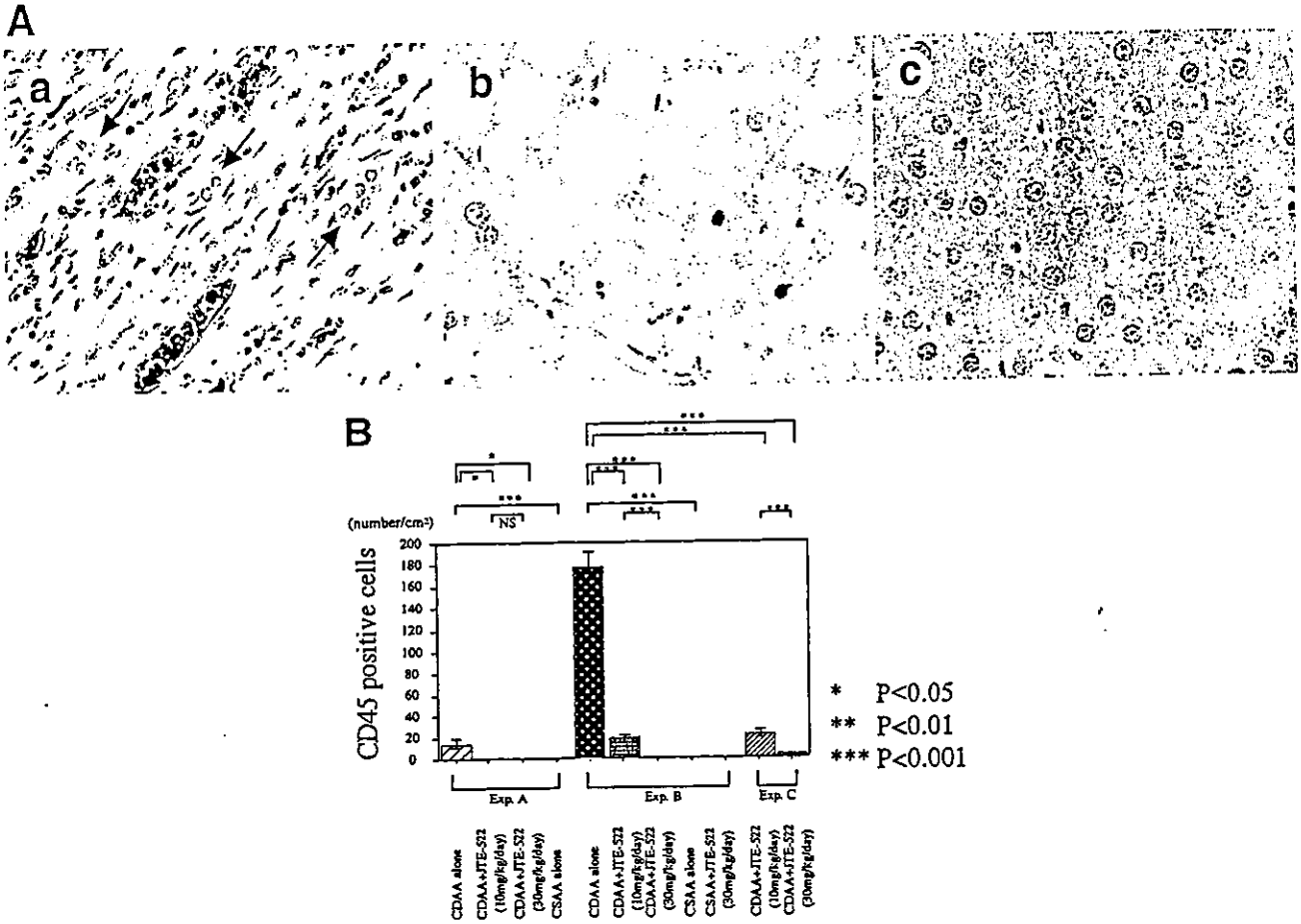


Figure 8. (*A*) Immunostaining for CD45 expression in the rat liver. (*a*) CDAA-treated rat liver for 36 weeks. CD45-positive inflammatory cells often appeared. *Arrows* indicate duct-like structure of hepatocytes and no inflammatory cells. Jurkat cells served as positive control (data not shown). (*b*) CDAA plus 10 mg · kg$^{-1}$ · day$^{-1}$ JTE-522 for 36 weeks. (*c*) CDAA plus 30 mg · kg$^{-1}$ · day$^{-1}$ JTE-522 for 36 weeks. (Original magnification 400×.) (*B*) Density of CD45-positive cells determined in all rats in experiments A–C. Data are mean ± SD.

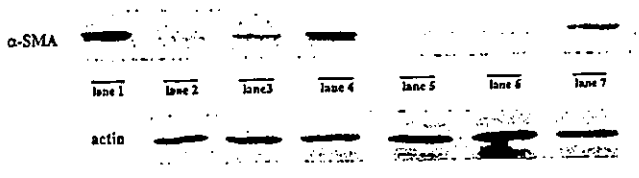


lane 1:Positive control
lane 2:CSAA (36 weeks)
lane 3:CDAA (12 weeks)
lane 4:CDAA (36weeks)
lane 5:CSAA + 30mg/kg/day JTE-522 (36 weeks)
lane 6:CDAA + 30mg/kg/day JTE-522 (36 weeks)
lane 7:CDAA + 10mg/kg/day JTE-522 (36 weeks)

Figure 9. Western blot for α-SMA expression in liver tissue. *Upper panel, lane 1*: positive control of human cirrhotic liver tissue; *lane 2*: CSAA (36 weeks); *lane 3*: CDAA (12 weeks); *lane 4*: CDAA (36 weeks); *lane 5*: CSAA containing 30 mg · kg$^{-1}$ · day$^{-1}$ JTE-522 (36 weeks); *lane 6*: CDAA containing 30 mg · kg$^{-1}$ · day$^{-1}$ JTE-522 (36 weeks); *lane 7*: CDAA containing 10 mg · kg$^{-1}$ · day$^{-1}$ JTE-522 (36 weeks). *Lower panel*: blots for actin served as loading controls.

further extension of the duration of the experiments. With regard to cancer development, it is notable that c-myc level was highly up-regulated in rat livers of the CDAA group, which is consistent with the previous report.[43] Interestingly, JTE-522 significantly decreased c-myc expression at a low dose and especially at a high dose, at least at the messenger RNA level, although the precise mechanism of HCC formation is not certain at present.

Western blot and immunohistochemistry showed that COX-2 was up-regulated from fibrous liver to cirrhosis in CDAA-treated groups. The mechanism(s) of COX-2 up-regulation is not known. However, it is postulated that transforming growth factor α is up-regulated in CDAA-treated rat liver and this molecule can induce COX-2 expression.[44,45] Alternatively, inflammation-associated cytokines such as tumor necrosis factor α and interleukin 1β can also induce COX-2.[46,47] By contrast, treatment with JTE-522 clearly decreased COX-2 expression dose dependently and the extent of liver fibrosis

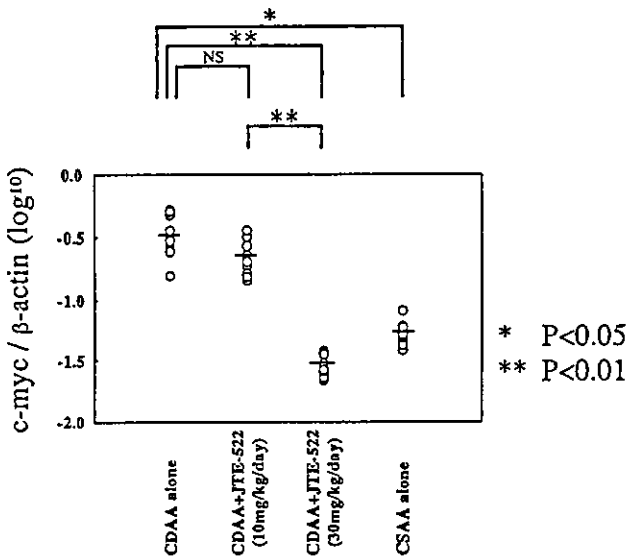


**Figure 10.** Quantitative reverse-transcription PCR for c-myc messenger RNA. c-myc messenger RNA levels in livers of rats fed CDAA for 36 weeks, CDAA plus low-dose JTE-522, CDAA plus high-dose JTE-522, and CSAA were measured by Light Cycler after reverse transcription. c-myc expression was normalized with rat β-actin expression. CDAA induced a high level of c-myc expression, and JTE-522 at a high dose significantly inhibited induction of c-myc gene expression.

was closely associated with COX-2 level (Figure *6B*). JTE-522–induced reduction of $PGE_2$ levels in the CDAA group ensured efficacy of the agent in vivo and suggests that COX-2–mediated arachidonate metabolism may play an essential role in the progression of rat fibrosis. However, we cannot exclude the possible involvement of targets other than COX-2 in this process.

CDAA-induced formation of preneoplastic lesions is mediated by a repeated sequence of liver cell necrosis and regenerative cell proliferation and probably involves oxidative DNA damage.[18,19] We found that the pathologic changes of liver correlated well with the extent of oxidative DNA damage as assessed by levels of 8-hydroxydeoxyguanosine (data not shown).[48] It appears that JTE-522 neutralized oxidative DNA damage and decreased transaminase levels through reduction of $PGE_2$ production. Although the precise mechanism of action of JTE-522 on the prevention of CDAA-induced fibrogenesis and hepatocarcinogenesis is not certain at present, our study provided several clues on the mechanism.

In both human and rat hepatocarcinogenesis, fibrosis is a major process that increases gradually from normal liver to cirrhosis. Activated hepatic stellate cells (also

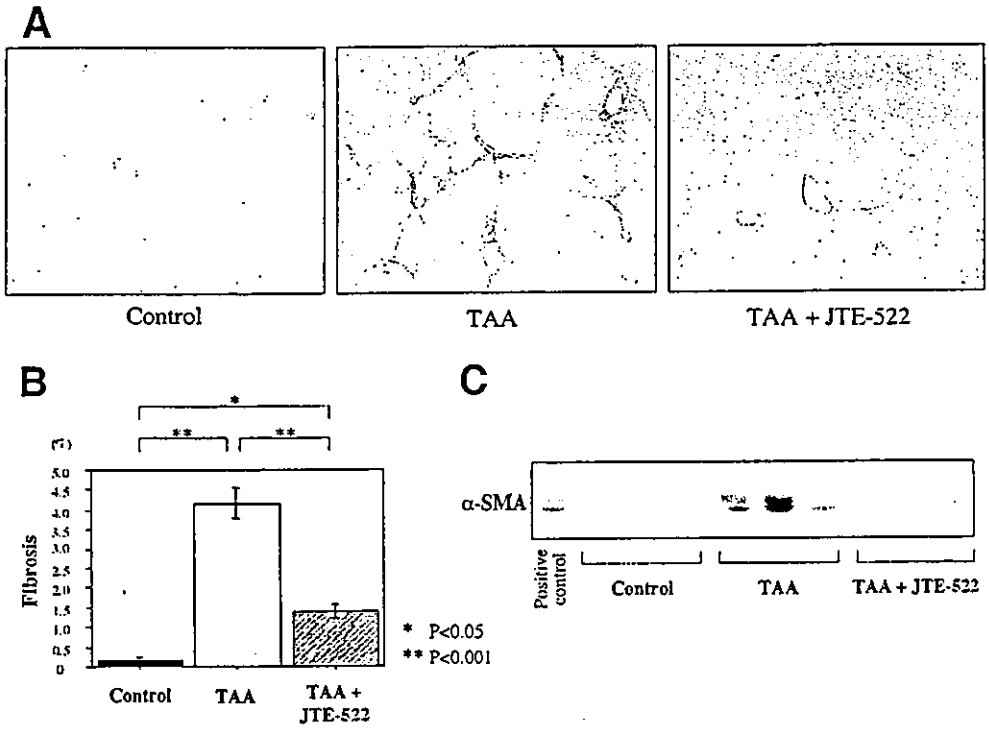


**Figure 11.** TAA-induced liver fibrosis model. (*A*) Collagen staining. TAA-treated rats showed marked liver fibrosis with pseudo-lobule formation, whereas TAA-treated rats administered JTE-522 (15 mg · $kg^{-1}$ · $day^{-1}$) show only weak fibrotic process in the liver. (*B*) Quantification of collagen staining. The difference between the TAA group and the TAA plus JTE-522 group was significant ($P < 0.001$). (*C*) Western blot analysis for α-SMA. TAA-treated fibrotic livers showed marked expression of α-SMA, and JTE-522 reduced the expression. Positive control: human cirrhotic liver tissue. Three representative samples for each group are shown. Equal loading of the proteins was confirmed by Ponso-S protein staining of the membrane (data not shown).

designated as fat-storing cells) are believed to play a crucial role in liver fibrogenesis, and collagen is the major component.[49] α-SMA is expressed by activated hepatic stellate cells but not by quiescent hepatic stellate cells; therefore, α-SMA serves as an appropriate marker for activated hepatic stellate cells.[20,32] Our results showed up-regulation of α-SMA from normal liver to fibrotic liver to cirrhosis and efficient suppression of α-SMA by JTE-522 in the CDAA group. The data suggest that JTE-522 may inhibit activation of hepatic stellate cells and lead to prevention of fibrogenesis. In vitro assay using hepatic stellate cell cultures may clarify this hypothesis.

Several studies indicate that COX-2 inhibitors suppress cell growth.[50,51] We previously found that JTE-522 had potent growth-suppressive effects on cholangiocellular carcinoma cells.[9] Therefore, it is assumed that this growth-suppressive effect of JTE-522 might lead to relatively slow regeneration of the proliferative hepatocytes, allowing a gradual process of fibrogenesis. We indeed found a low proliferative activity in JTE-522–treated livers as assessed by PCNA staining. Alternatively, choline deficiency is known to induce hepatocyte apoptosis in vitro and in vivo.[52] Although inhibition of COX-2 can induce apoptosis in several cell culture systems, recent studies indicate that the COX-2 inhibitor rather blocks apoptotic pathway in certain situations.[53,54] This possibility should be also considered.

Another possibility is that the anti-inflammatory effects of JTE-522 might contribute to repression of persistent inflammation and ultimately lead to a reduction of fibrogenesis. It is known that persistent inflammation promotes human liver fibrogenesis, as often seen in hepatitis C virus–infected liver.[55] By histologic examination of livers in the CDAA group, we found that infiltrative inflammatory cells appeared in liver fibrosis and cirrhotic livers had quite severe inflammation. This finding was further confirmed by CD45 staining that could detect all types of leukocytes. It should be emphasized here that CDAA-induced liver fibrosis in rats is substantially different from hepatitis C virus–based fibrosis with respect to the underlying pathologic process (e.g., oxidative DNA damage vs. viral infection). However, the present findings of PCNA expression, activated hepatic stellate cells, and liver inflammation in our rat CDAA model are of potential importance because dysregulation of these parameters is also seen in human liver fibrosis.[32,49,55,56]

We focused on the effect and mechanism of JTE-522–mediated inhibition of CDAA-induced liver fibrosis, but does this compound inhibit liver fibrogenesis in a mechanistically distinct form of liver disease? To address this question, we performed additional experiments using the TAA-induced liver fibrosis model. Our results showed that, even with a moderate dose (15 $mg \cdot kg^{-1} \cdot day^{-1}$), JTE-522 also inhibited liver fibrosis in TAA-treated rats when estimated by collagen staining and α-SMA expression. Although the underlined mechanism of the protective effect of JTE-522 against TAA-induced fibrosis should be explored in the next stage, the results at least indicate that JTE-522–mediated inhibition of liver fibrosis is rather a universal effect and is not limited to the CDAA model alone.

In conclusion, the present study suggests that COX-2 may be the principal enzyme involved in the development of rat experimental liver fibrosis and that JTE-522 is an effective chemopreventive agent with low toxicity.

## References


1. Landis SH, Murray T, Bolden S, Wingo PA. Cancer statistics, 1998. CA Cancer J Clin 1998;48:6–29.
2. Ikeda K, Saitoh S, Koida I, Arase Y, Tsubota A, Chayama K, Kumada H, Kawanishi M. A multivariate analysis of risk factors for hepatocellular carcinogenesis: a prospective observation of 795 patients with viral and alcoholic cirrhosis. Hepatology 1993; 18:47–53.
3. Hla T, Neilson K. Human cyclooxygenase-2 cDNA. Proc Natl Acad Sci U S A 1992;89:7384–7388.
4. DuBois RN, Awad J, Morrow J, Roberts LJ 2nd, Bishop PR. Regulation of eicosanoid production and mitogenesis in rat intestinal epithelial cells by transforming growth factor-alpha and phorbol ester. J Clin Invest 1994;93:493–498.
5. Singer II, Kawka DW, Schloemann S, Tessner T, Riehl T, Stenson WF. Cyclooxygenase 2 is induced in colonic epithelial cells in inflammatory bowel disease. Gastroenterology 1998;115:297–306.
6. Dannenberg AJ, Altorki NK, Boyle JO, Dang C, Howe LR, Weksler BB, Subbaramaiah K. Cyclo-oxygenase 2: a pharmacological target for the prevention of cancer. Lancet Oncol 2001;2:544–551.
7. Koga H, Sakisaka S, Ohishi M, Kawaguchi T, Taniguchi E, Sasatomi K, Harada M, Kusaba T, Tanaka M, Kimura R, Nakashima Y, Nakashima O, Kojiro M, Kurohiji T, Sata M. Expression of cyclooxygenase-2 in human hepatocellular carcinoma: relevance to tumor dedifferentiation. Hepatology 1999;29:688–696.
8. Kondo M, Yamamoto H, Nagano H, Okami J, Ito Y, Shimizu J, Eguchi H, Miyamoto A, Dono K, Umeshita K, Matsuura N, Wakasa K, Nakamori S, Sakon M, Monden M. Increased expression of COX-2 in nontumor liver tissue is associated with shorter disease-free survival in patients with hepatocellular carcinoma. Clin Cancer Res 1999;5:4005–4012.
9. Hayashi N, Yamamoto H, Hiraoka N, Dono K, Ito Y, Okami J, Kondo M, Nagano H, Umeshita K, Sakon M, Matsuura N, Nakamori S, Monden M. Differential expression of cyclooxygenase-2 (COX-2) in human bile duct epithelial cells and bile duct neoplasm. Hepatology 2001;34:638–650.
10. Oshima M, Dinchuk JE, Kargman SL, Oshima H, Hancock B, Kwong E, Trzaskos JM, Evans JF, Taketo MM. Suppression of intestinal polyposis in Apc delta716 knockout mice by inhibition of cyclooxygenase 2 (COX-2). Cell 1996;87:803–809.
11. Reddy BS, Rao CV, Seibert K. Evaluation of cyclooxygenase-2 inhibitor for potential chemopreventive properties in colon carcinogenesis. Cancer Res 1996;56:4566–4569.
12. Steinbach G, Lynch PM, Phillips RK, Wallace MH, Hawk E, Gordon GB, Wakabayashi N, Saunders B, Shen Y, Fujimura T, Su LK,

Levin B. The effect of celecoxib, a cyclooxygenase-2 inhibitor, in familial adenomatous polyposis. N Engl J Med 2000;342:1946–1952.
13. Matsushita M, Masaki M, Yagi Y, Tanaka T, Wakitani K. Pharmacological profile of JTE-522, a novel prostaglandin H synthase-2 inhibitor, in rats. Inflamm Res 1997;46:461–466.
14. Wakitani K, Nanayama T, Masaki M, Matsushita M. Profile of JTE-522 as a human cyclooxygenase-2 inhibitor. Jpn J Pharmacol 1998;78:365–371.
15. Sasai H, Masaki M, Wakitani K. Suppression of polypogenesis in a new mouse strain with a truncated Apc (Delta474) by a novel COX-2 inhibitor, JTE-522. Carcinogenesis 2000;21:953–958.
16. Tomozawa S, Nagawa H, Tsuno N, Hatano K, Osada T, Kitayama J, Sunami E, Nita ME, Ishihara S, Yano H, Tsuruo T, Shibata Y, Muto T. Inhibition of haematogenous metastasis of colon cancer in mice by a selective COX-2 inhibitor, JTE-522. Br J Cancer 1999;81:1274–1279.
17. Li Z, Shimada Y, Kawabe A, Sato F, Maeda M, Komoto I, Hong T, Ding Y, Kaganoi J, Imamura M. Suppression of N-nitrosomethylbenzylamine (NMBA)-induced esophageal tumorigenesis in F344 rats by JTE-522, a selective COX-2 inhibitor. Carcinogenesis 2001;22:547–551.
18. Denda A, Endoh T, Kitayama W, Tang Q, Noguchi O, Kobayashi Y, Akai H, Okajima E, Tsujiuchi T, Tsutsumi M, Nakae D, Konishi Y. Inhibition by piroxicam of oxidative DNA damage, liver cirrhosis and development of enzyme-altered nodules caused by a choline-deficient, L-amino acid-defined diet in rats. Carcinogenesis 1997; 18:1921–1930.
19. Denda A, Endoh T, Tang Q, Tsujiuchi T, Nakae D, Konishi Y. Prevention by inhibitors of arachidonic acid cascade of liver carcinogenesis, cirrhosis and oxidative DNA damage caused by a choline-deficient, L-amino acid-defined diet in rats. Mutat Res 1998;402:279–288.
20. Ikejima K, Takei Y, Honda H, Hirose M, Yoshikawa M, Zhang Y-J, Lang T, Fukuda T, Yamashina S, Kitamura T, Sato N. Leptin receptor-mediated signaling regulates hepatic fibrogenesis and remodeling of extracellular matrix in the rat. Gastroenterology 2002;122:1399–1410.
21. El-Bayoumy K, Iatropoulos M, Amin S, Hoffmann D, Wynder EL. Increased expression of cyclooxygenase-2 in rat lung tumors induced by the tobacco-specific nitrosamine 4-(methylnitrosamino)-4-(3-pyridyl)-1-butanone: the impact of a high-fat diet. Cancer Res 1999;59:1400–1403.
22. Satoh K, Kitahara A, Soma Y, Inaba Y, Hatayama I, Sato K. Purification, induction, and distribution of placental glutathione transferase: a new marker enzyme for pre-neoplastic cells in the rat chemical hepatocarcinogenesis. Proc Natl Acad Sci U S A 1985;82:3964–3968.
23. Schmitt-Graff A, Kruger S, Bochard F, Gabbiani G, Denk H. Modulation of alpha smooth muscle actin and desmin expression in perisinusoidal cells of normal and diseased human livers. Am J Pathol 1991;138:1233–1242.
24. Sunderland CA, McMaster WR, Williams AF. Purification with monoclonal antibody of a predominant leukocyte-common antigen and glycoprotein from rat thymocytes. Eur J Immunol 1979; 9:155–159.
25. Yamashita N, Minamoto T, Onda M, Esumi H. Increased cell proliferation of azoxymethane-induced aberrant crypt foci of rat colon. Jpn J Cancer Res 1994;85:692–698.
26. Sugihara A, Tsujimura T, Fujita Y, Nakata Y, Terada N. Evaluation of role of mast cells in the development of liver fibrosis using mast cell-deficient rats and mice. J Hepatol 1999;30:859–867.
27. Squire RA, Levitt MH. Report of a workshop on classification of specific hepatocellular lesions in rats. Cancer Res 1975;35: 3214–3223.
28. Yamamoto H, Soh JW, Shirin H, Xing WQ, Lim JT, Yao Y, Slosberg E, Tomita N, Schieren I, Weinstein IB. Comparative effects of overexpression of p27Kip1 and p21Cip1/Waf1 on growth and differentiation in human colon carcinoma cells. Oncogene 1999; 18:103–115.
29. Miyata H, Doki Y, Yamamoto H, Kishi K, Takemoto H, Fujiwara Y, Yasuda T, Yano M, Inoue M, Shiozaki H, Weinstein IB, Monden M. Overexpression of CDC25B overrides radiation-induced G2-M arrest and results in increased apoptosis in esophageal cancer cells. Cancer Res 2001;61:3188–3193.
30. Fujiwara Y, Ooka M, Sugita Y, Sakita I, Tamaki Y, Monden M. Prevention of cross-contamination during sampling procedure in molecular detection for cancer micrometastasis. Cancer Lett 2000;153:109–111.
31. Sandhu H, Dehnen W, Roller M, Abel J, Unfried K. mRNA expression patterns in different stages of asbestos-induced carcinogenesis in rats. Carcinogenesis 2000;21:1023–1029.
32. Friedman SL. Seminars in medicine of the Beth Israel Hospital, Boston. The cellular basis of hepatic fibrosis. Mechanisms and treatment strategies. N Engl J Med 1993;328:1828–1835.
33. Denda A, Tang Q, Endoh T, Tsujiuchi T, Horiguchi K, Noguchi O, Mizumoto Y, Nakae D, Konishi Y. Prevention by acetylsalicylic acid of liver cirrhosis and carcinogenesis as well as generations of 8-hydroxydeoxyguanosine and thiobarbituric acid-reactive substances caused by a choline-deficient, L-amino acid-defined diet in rats. Carcinogenesis 1994;15:1279–1283.
34. Weinblatt ME. Nonsteroidal anti-inflammatory drug toxicity: increased risk in the elderly. Scand J Rheumatol 1991;91:9–17.
35. Bosch-Marce M, Claria J, Titos E, Masferrer JL, Altuna R, Poo JL, Jimenez W, Arroyo V, Rivera F, Rodes J. Selective inhibition of cyclooxygenase 2 spares renal function and prostaglandin synthesis in cirrhotic rats with ascites. Gastroenterology 1999;116: 1167–1175.
36. Goldstein JL, Silverstein FE, Agrawal NM, Hubbard RC, Kaiser J, Maurath CJ, Verburg KM, Geis GS. Reduced risk of upper gastrointestinal ulcer complications with celecoxib, a novel COX-2 inhibitor. Am J Gastroenterol 2000;95:1681–1690.
37. Moore MA, Nakagawa K, Satoh K, Ishikawa T, Sato K. Single GST-P positive liver cells—putative initiated hepatocytes. Carcinogenesis 1987;8:483–486.
38. Okajima E, Denda A, Ozono S, Takahama M, Akai H, Sasaki Y, Kitayama W, Wakabayashi K, Konishi Y. Chemopreventive effects of nimesulide, a selective cyclooxygenase-2 inhibitor, on the development of rat urinary bladder carcinomas initiated by N-butyl-N-(4-hydroxybutyl)nitrosamine. Cancer Res 1998;58: 3028–3031.
39. Nakatsugi S, Ohta T, Kawamori T, Mutoh M, Tanigawa T, Watanabe K, Sugie S, Sugimura T, Wakabayashi K. Chemoprevention by nimesulide, a selective cyclooxygenase-2 inhibitor, of 2-amino-1-methyl-6-phenylimidazo [4,5-b]pyridine (PhIP)-induced mammary gland carcinogenesis in rats. Jpn J Cancer Res 2000; 91:886–892.
40. Shiotani H, Denda A, Yamamoto K, Kitayama W, Endoh T, Sasaki Y, Tsutsumi N, Sugimura M, Konishi Y. Increased expression of cyclooxygenase-2 protein in 4-nitroquinoline-1-oxide-induced rat tongue carcinomas and chemopreventive efficacy of a specific inhibitor, nimesulide. Cancer Res 2001;61:1451–1456.
41. Kawamori T, Rao CV, Seibert K, Reddy BS. Chemopreventive activity of celecoxib, a specific cyclooxygenase-2 inhibitor, against colon carcinogenesis. Cancer Res 1998;58:409–412.
42. Grubbs CJ, Lubet RA, Koki AT, Leahy KM, Masferrer JL, Steele VE, Kelloff GJ, Hill DL, Seibert K. Celecoxib inhibits N-butyl-N-(4-hydroxybutyl)-nitrosamine-induced urinary bladder cancers in male B6D2F1 mice and female Fischer-344 rats. Cancer Res 2000;60:5599–5602.
43. Chandar N, Lombardi B, Locker J. c-myc gene amplification during hepatocarcinogenesis by a choline-devoid diet. Proc Natl Acad Sci U S A 1989;86:2703–2707.
44. Masuhara M, Katyal SL, Nakamura T, Shinozuka H. Differential

expression of hepatocyte growth factor, transforming growth factor-alpha and transforming growth factor-beta 1 messenger RNAs in two experimental models of liver cell proliferation. Hepatology 1992;16:1241–1249.
45. Matsuura H, Sakaue M, Subbaramaiah K, Kamitani H, Eling TE, Dannenberg AJ, Tanabe T, Inoue H, Arata J, Jetten AM. Regulation of cyclooxygenase-2 by interferon gamma and transforming growth factor alpha in normal human epidermal keratinocytes and squamous carcinoma cells. Role of mitogen-activated protein kinases. J Biol Chem 1999;274:29138–29148.
46. Arias-Negrete S, Keller K, Chadee K. Proinflammatory cytokines regulate cyclooxygenase-2 mRNA expression in human macrophages. Biochem Biophys Res Commun 1995;208:582–589.
47. Feng L, Xia Y, Garcia GE, Hwang D, Wilson CB. Involvement of reactive oxygen intermediates in cyclooxygenase-2 expression induced by interleukin-1, tumor necrosis factor-alpha, and lipopolysaccharide. J Clin Invest 1995;95:1669–1675.
48. Fraga CG, Shigenaga MK, Park JW, Degan P, Ames BN. Oxidative damage to DNA during aging: 8-hydroxy-2'-deoxyguanosine in rat organ DNA and urine. Proc Natl Acad Sci U S A 1990;87:4533–4537.
49. Maher JJ, McGuire RF. Extracellular matrix gene expression increases preferentially in rat lipocytes and sinusoidal endothelial cells during hepatic fibrosis in vivo. J Clin Invest 1990;86:1641–1648.
50. Sheng H, Shao J, Kirkland SC, Isakson P, Coffey RJ, Morrow J, Beauchamp RD, DuBois RN. Inhibition of human colon cancer cell growth by selective inhibition of cyclooxygenase-2. J Clin Invest 1997;99:2254–2259.
51. Goldman AP, Williams CS, Sheng H, Lamps LW, Williams VP, Pairet M, Morrow JD, DuBois RN. Meloxicam inhibits the growth of colorectal cancer cells. Carcinogenesis 1998;19:2195–2199.
52. Albright CD, Zeisel SH. Choline deficiency causes increased localization of transforming growth factor-beta1 signaling proteins and apoptosis in the rat liver. Pathobiology 1997;65:264–270.
53. Munkarah AR, Genhai Z, Morris R, Baker VV, Deppe G, Diamond MP, Saed GM. Inhibition of paclitaxel-induced apoptosis by the specific COX-2 inhibitor, NS398, in epithelial ovarian cancer cells. Gynecol Oncol 2003;88:429–433.
54. Na HK, Surh YJ. Induction of cyclooxygenase-2 in Ras-transformed human mammary epithelial cells undergoing apoptosis. Ann N Y Acad Sci 2002;973:153–160.
55. Seeff LB. Natural history of hepatitis C. Am J Med 1999;107:10S–15S.
56. Kawakita N, Seki S, Sakaguchi H, Yanai A, Kuroki T, Mizoguchi Y, Kobayashi K, Monna T. Analysis of proliferating hepatocytes using a monoclonal antibody against proliferating cell nuclear antigen/cyclin in embedded tissues from various liver diseases fixed in formaldehyde. Am J Pathol 1992;140:513–520.

Received January 15, 2002. Accepted May 15, 2003.

Address requests for reprints to: Hirofumi Yamamoto, M.D., Ph.D., Department of Surgery and Clinical Oncology, Graduate School of Medicine, Osaka University, 2-2 Yamada-oka, Suita-City, Osaka 565-0871, Japan. e-mail: kobunyam@surg2.med.osaka-u.ac.jp; fax: (81) 6-6879-3259.

Supported by grants in aid from the Ministry of Education, Science, Sports and Culture and from the Ministry of Health and Welfare, Japan, and in part by a grant-in-aid from the Second Term Comprehensive 10-Year Strategy for Cancer Control (H12-Cancer-020) and Cancer Research.

The authors thank Y. Naito and S. Yamane for preparation of numerous paraffin sections; S. Hayashi, I. Seshimo, H. Ota, and S. Yamamoto for staining and pathologic works; and K. Goto and M. Kubota for animal experiments.

H.Y. and M.K. contributed equally to this work.

*Annals of Surgical Oncology*, 10(10):1184–1190
DOI: 10.1245/ASO.2003.03.010

# Interferon-$\beta$ Is More Potent Than Interferon-$\alpha$ in Inhibition of Human Hepatocellular Carcinoma Cell Growth When Used Alone and in Combination With Anticancer Drugs

Bazarragchaa Damdinsuren, MD, Hiroaki Nagano, PhD, Masato Sakon, PhD, Motoi Kondo, PhD, Tameyoshi Yamamoto, MD, Koji Umeshita, PhD, Keizo Dono, PhD, Shoji Nakamori, PhD, and Morito Monden, PhD

**Background:** The prognosis of advanced hepatocellular carcinoma (HCC) is extremely poor, but promising effects of chemotherapies combined with interferon (IFN) have been reported.

**Methods:** To develop more effective combination therapies for HCC, we compared the antiproliferative effects of IFN-$\alpha$ and IFN-$\beta$ in combination with various cytotoxic drugs on hepatoma cell lines using MTT assay and isobologram analysis.

**Results:** IFN-$\beta$ was more potent than IFN-$\alpha$ in inhibiting the cell growth of all cell lines ($P < .05$, two-way ANOVA). PLC/PRF/5 was more sensitive to either IFN, than HLE and HuH7. Cell growth of all cell lines was inhibited in a dose-dependent manner by 5-fluorouracil (5-FU), cisplatin (CDDP), and doxorubicin (DOX), but the sensitivities of these cells were considerably different. As for IFN-$\alpha$, synergistic effects were observed when combined with 5-FU and DOX on PLC/PRF/5 cells only, whereas IFN-$\beta$ showed synergistic effects with 5-FU and CDDP on HuH7 and PLC/PRF/5 cell lines.

**Conclusion:** The spectra of the antiproliferative activity and synergistic effect of IFN-$\beta$ when combined with anticancer drugs are more potent than those of IFN-$\alpha$. Combinations of IFN-$\beta$ and anticancer drugs may provide a better treatment of HCC when combinations with IFN-$\alpha$ are ineffective.

**Key Words:** Interferon—Anticancer drug—Cell proliferation—HCC—Combination therapy.

Hepatocellular carcinoma (HCC) is a common malignancy worldwide, and half a million new cases are diagnosed every year.[1–3] Despite recent advances in diagnostic modalities for HCC, more than 80% of the new cases are diagnosed in the inoperable, advanced stages of the disease. Unfortunately, the prognosis of such patients is extremely poor, with a 5-year survival of <10%,[4,5] and no standard treatment is available for such cases.

Although various chemotherapies have been used for the treatment of HCC, chemotherapeutic agents are generally not effective either when used alone or in combination therapy with other drugs.[5] However, recent clinical trials suggested that combination therapy with chemotherapeutic agents and interferon (IFN)-$\alpha$ may be effective against advanced HCCs,[6] including those showing tumor invasion into the major branches of the portal vein.[7,8] However, other investigators have reported the ineffectiveness of some of such regimens,[9] thus necessitating the need for more effective combination therapies with IFN.

IFNs consist of type I IFN, which includes IFN-$\alpha$, -$\beta$, -$\omega$, and type II IFN, also known as IFN-$\gamma$.[10] Although the antiproliferative effects of IFN-$\alpha$ and -$\gamma$ have been studied in detail in various cell types, those of IFN-$\beta$ are not

Received March 6, 2003; accepted August 25, 2003.

From the Department of Surgery and Clinical Oncology (E2), Graduate School of Medicine, Osaka University, Osaka, Japan.

Presented at the 56th Annual Cancer Symposium of the Society of Surgical Oncology, Los Angeles, California, March 5–9, 2003.

Address correspondence and reprint requests to: Masato Sakon, PhD, Department of Surgery and Clinical Oncology (E2), Graduate School of Medicine, Osaka University, 2-2, Yamadaoka, Suita, Osaka 565–0871, Japan; Fax: 81-6-6879-3259; E-mail: msakon@surg2.med.osaka-u.ac.jp

well understood, especially when it is combined with anticancer drugs. It is also not clear how IFNs modulate the antitumor activity of anticancer drugs in HCC cells.

The present study was designed to compare the antiproliferative effects of IFN-$\alpha$ and -$\beta$, and of their combinations with chemotherapeutic agents [5-fluorouracil (5-FU), cisplatin (CDDP), and doxorubicin (DOX)] on three hepatoma cell lines, in order to develop a more effective combination therapy for HCC.

## MATERIALS AND METHODS

### Cell Lines

Three human HCC cell lines, including HLE, HuH7, and PLC/PRF/5, were purchased from the Japanese Cancer Research Resources Bank (Tokyo, Japan). They were maintained in Dulbecco's Modified Eagle Medium supplemented with 10% fetal bovine serum, 100 units/mL penicillin, and 100 $\mu$g/mL streptomycin at 37°C in humidified incubator with 5% $CO_2$ in air.

### Drugs and Reagents

Purified human lymphoblast IFN-$\alpha$ (OIF) was kindly supplied by Otsuka Pharmaceutical Co. (Tokushima, Japan), and its activity was approximately $2.12 \times 10^8$ IU/mg. Human natural fibroblast IFN-$\beta$ (IFN$\beta$ Mochida) was provided by Mochida Pharmaceutical Co. (Tokyo, Japan), with a specific activity of $3.7 \times 10^8$ IU/mg. 5-FU (Fluorouracil) and DOX (Adriacin) were obtained from Kyowa Hakko Co. (Tokyo), and CDDP (Randa) was purchased from Nippon Kayaku Co. (Tokyo). All drugs were stored at −20°C, and the stock solutions were constituted in distilled water. The concentration of the final compound in the culture medium never exceeded 0.1% in treated samples. MTT (3-[4,5-dimethylthiazol-2yl]-2,5-diphenyltetrazolium bromide) was obtained from Sigma Co. (St. Louis, MO).

### Growth Inhibition Assays

Cells ($3 \times 10^3$/well) were added in triplicate to a 96-well microplate. The medium was replaced 24 hours later by 0.1 mL of fresh medium containing various concentrations of IFN-$\alpha$ or -$\beta$, with or without different concentrations of 5-FU, CDDP, or DOX. In combination experiments, the test concentrations of IFN-$\alpha$ were 50 and 500 IU/mL, IFN-$\beta$ were 50, 500, and 5000 IU/mL, and those of 5-FU were .05, .5, and 5 $\mu$g/mL, CDDP .1, .5, and 1 $\mu$g/mL, and DOX .01, .1, and 1 $\mu$g/mL. The concentrations of IFNs in growth-inhibitory assays for IFN alone were 50, 500, 5.000, and 25.000 IU/mL. Tumor cells suspended in complete medium were used as a control for cell viability. The medium was changed every 48 hours, and 4 days after the addition of drugs, the number of viable cells was assessed by MTT (Sigma) assay. Briefly, 10 $\mu$L (50 $\mu$g) of MTT were added to each well, and the plate was incubated for 4 hours at 37°C. Unreacted MTT was then removed, leaving the resultant formazan crystals at the bottom of the well. Then, 0.1 mL of 2-propanol was added to each well to dissolve the crystal. The absorbance of the plate was measured in a microplate reader at a wavelength of 570 nm, and the results were expressed as the percentage of absorbance relative to untreated controls. These assays were repeated at least 3 times, and similar results were obtained.

### Evaluation of Cooperative Effects

Synergy of cooperative cytotoxicity was determined by isobole analysis as described by Berenbaum.[11] The effect of a particular dose combination for two agents $A$ and $B$ was determined by applying the equation: $Ac/Ae + Bc/Be = D$, where $Ac$ and $Bc$ correspond to the concentrations of the drugs used in the combination treatment, $Ae$ and $Be$ correspond to the concentrations of the drugs that could produce alone the same magnitude of effect. When $D$ (combination index) $< .8$, the effect of the combination was synergistic, whereas when ($.8 \leq D < 1.2$) or $D \geq 1.2$, the effect was additive or antagonistic, respectively. Drug potentiation was calculated as the amount of the drug used alone to yield the same effect as the drug in combination divided by the amount of the drug used in the combination.

### Statistical Analyses

Statistical analyses were performed using the StatView J-5.0 program (Abacus Concepts Inc., Berkeley, CA). Data are expressed as average of at least three independent experiments, unless stated otherwise. The Mann-Whitney test was used to examine the differences between drug combination groups. The significance of differences of IFNs growth-inhibitory effect or the sensitivities of the cell lines to IFN was calculated by two-way ANOVA. In all analyses, values of $P < .05$ were considered statistically significant.

## RESULTS

### Antiproliferative Effects of IFN-$\alpha$ and IFN-$\beta$

The effects of IFN-$\alpha$ and -$\beta$ on cell growth were compared in three human HCC cell lines (HLE, HuH7, and PLC/PRF/5) (Fig. 1). The growth-inhibitory effect of IFN-$\beta$ was significantly more potent than that of IFN-$\alpha$ in all cell lines ($P < .05$, by two-factor ANOVA). The 50% growth-inhibition concentrations ($EC_{50}$) of IFN-$\beta$ and IFN-$\alpha$ on PLC/PRF/5 cells were $1.08 \times 10^{-3}$ and $31.13 \times 10^{-3}$

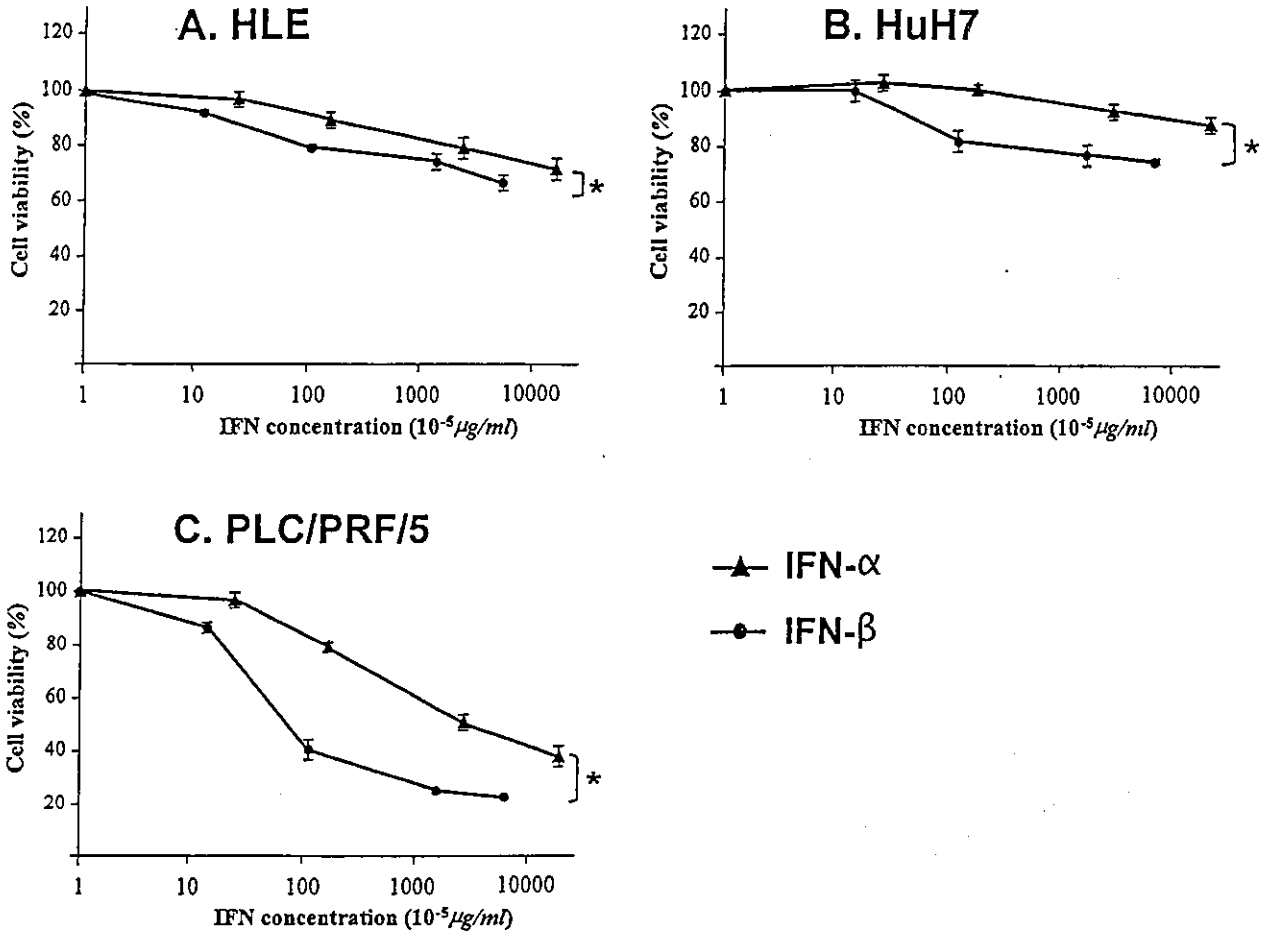


FIG. 1. Growth-inhibitory effects of IFN-$\alpha$ and -$\beta$ on HCC cell lines. (A) HuH7, (B) PLC/PRF/5, and (C) HLE cells were incubated for 4 days and cell viability was determined as described in Materials and Methods. Proportion of viable cells incubated without IFNs was considered 100%. Data are mean ± SEM of 4 independent experiments. *$P < .05$, statistical comparison was performed by two-way ANOVA.

$\mu$g/mL, respectively, where the antiproliferative effect of the former was 29-fold stronger than the latter.

The sensitivity of cultured cells to the two IFNs was considerably different. No or weak growth-inhibitory effect was observed in HuH7 and HLE cell lines by IFN-$\alpha$ up to high concentration (where growth inhibition by 20% compared to controls for HuH7 cells were $117.9 \times 10^{-3}$ and $2.7 \times 10^{-3}$ $\mu$g/ml, or for HLE $18.9 \times 10^{-3}$ $\mu$g/ml and $1.2 \times 10^{-3}$ $\mu$g/mL, for IFN-$\alpha$ and IFN-$\beta$, respectively), whereas PLC/PRF/5 cells were highly sensitive to both IFNs (where the above growth inhibition effect was reached by $2.7 \times 10^{-3}$ $\mu$g/mL of IFN-$\alpha$ or by $.3 \times 10^{-3}$ $\mu$g/mL of IFN-$\beta$).

### Antiproliferative Effects of Combination Treatment of IFNs and Anticancer Drugs

Growth-inhibitory assays were performed to investigate whether IFNs enhance the antiproliferative effects of anticancer drugs on HCC cell lines. The concentrations of chemotherapeutic drugs were selected based on the $EC_{50}$ of the drugs (data not shown) and the results of previous studies.[12]

5-FU exhibited a dose-dependent growth-inhibitory effect on all cell lines (Fig. 2) except HLE cells (left panels). When 5-FU and IFN-$\alpha$ were administered simultaneously, the antiproliferative effects were higher than those of each drug alone in PLC/PRF/5 cells (Fig. 2A). IFN-$\beta$ also enhanced the growth-inhibitory effects of 5-FU in a dose-dependent manner in all cell lines (Fig. 2B).

CDDP also showed dose-dependent antitumor effects in all cell lines (Fig. 3). The growth inhibition by CDDP was highest in HLE and lowest in PLC/PRF/5 cells. Concurrent application of IFN-$\alpha$ did not increase the antiproliferative effects of CDDP (Fig. 3A), whereas IFN-$\beta$ clearly improved the dose-dependent inhibitory effects of CDDP (Fig. 3B).

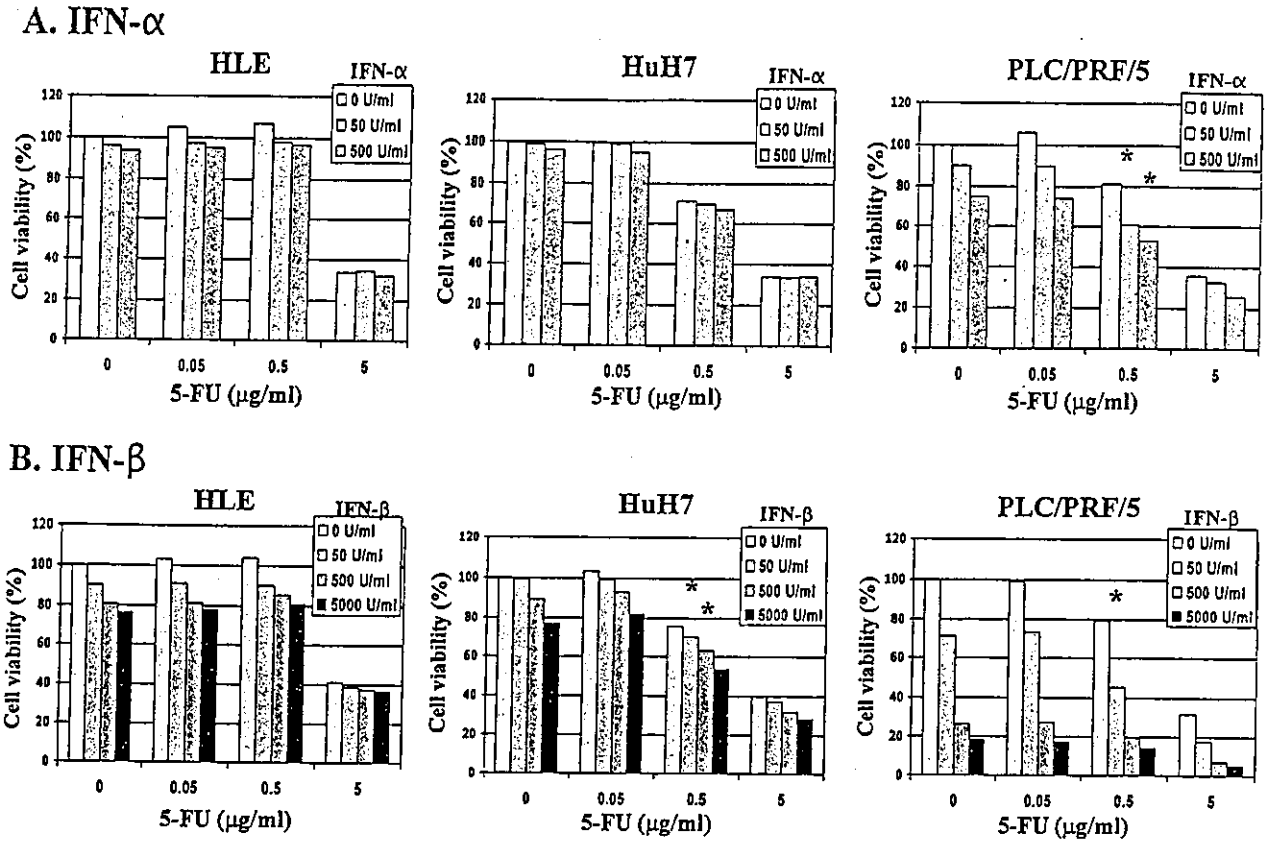


FIG. 2. Growth-inhibitory effects of IFN-$\alpha$ and -$\beta$ in combination of various doses of 5-fluorouracil (5-FU). Cells were incubated with IFN-$\alpha$ (A) or IFN-$\beta$ (B) in the presence of various concentrations of 5-FU and cell proliferation was determined on day 4, as described in Materials and Methods. Proportion of viable cells incubated without drugs was considered 100%. Data are the average of 3 independent experiments. *$P < .05$, denote significant synergistic effect, as examined by isobologram analysis.

The antiproliferative effects of DOX were diverse in the cell lines, showing higher cytotoxicity in HuH7 and HLE and weaker in PLC/PRF/5 cells (Fig. 4). Coincubation of IFN-$\alpha$ or IFN-$\beta$ with DOX enhanced the antiproliferative effects on PLC/PRF/5 cells, but not HLE and HuH7 cells.

### Cooperative Effects of IFNs and Anticancer Drugs

The isobologram analysis was performed for each combination of IFNs and anticancer drugs as described in Materials and Methods, and the results are summarized in Table 1. The cooperative growth-inhibitory patterns were different between combinations of IFN-$\alpha$ and those of IFN-$\beta$. The latter exhibited more synergistic cooperative effects in HuH7 and PLC/PRF/5. The synergistic effect was observed in PLC/PRF/5 cells in combinations of IFN-$\alpha$ (50–500 IU/mL) plus 5-FU (.5 $\mu$g/mL), and IFN-$\alpha$ (50 IU/mL) plus DOX (.1 $\mu$g/mL). On the other hand, IFN-$\beta$ (50 and /or 500 IU/mL) showed a synergistic effect with 5-FU (.5 $\mu$g/mL) and CDDP (.5 or .1 $\mu$g/mL concentrations) in HuH7 and PLC/PRF/5 cells. In fact, the combinations with IFN-$\alpha$ or IFN-$\beta$ exhibited additive or antagonistic cooperative effects on HLE cell line.

## DISCUSSION

The clinical efficacy of combination chemotherapy with IFN-$\alpha$ has already been reported.[6–8] The response rate of these therapies ranged from 26% to 63% of selected patients with highly advanced HCCs, suggesting that the remaining patients did not respond to the therapy and died within a few months. To develop more effective combination immunochemotherapy for HCC, in the present study, we examined the cooperative effects of two IFNs: -$\alpha$ and -$\beta$, with anticancer drugs, on human hepatoma cell lines using growth-inhibitory assays and isobologram analyses. Our results demonstrated that the growth-inhibitory effects of IFN-$\beta$ on HCC cells were

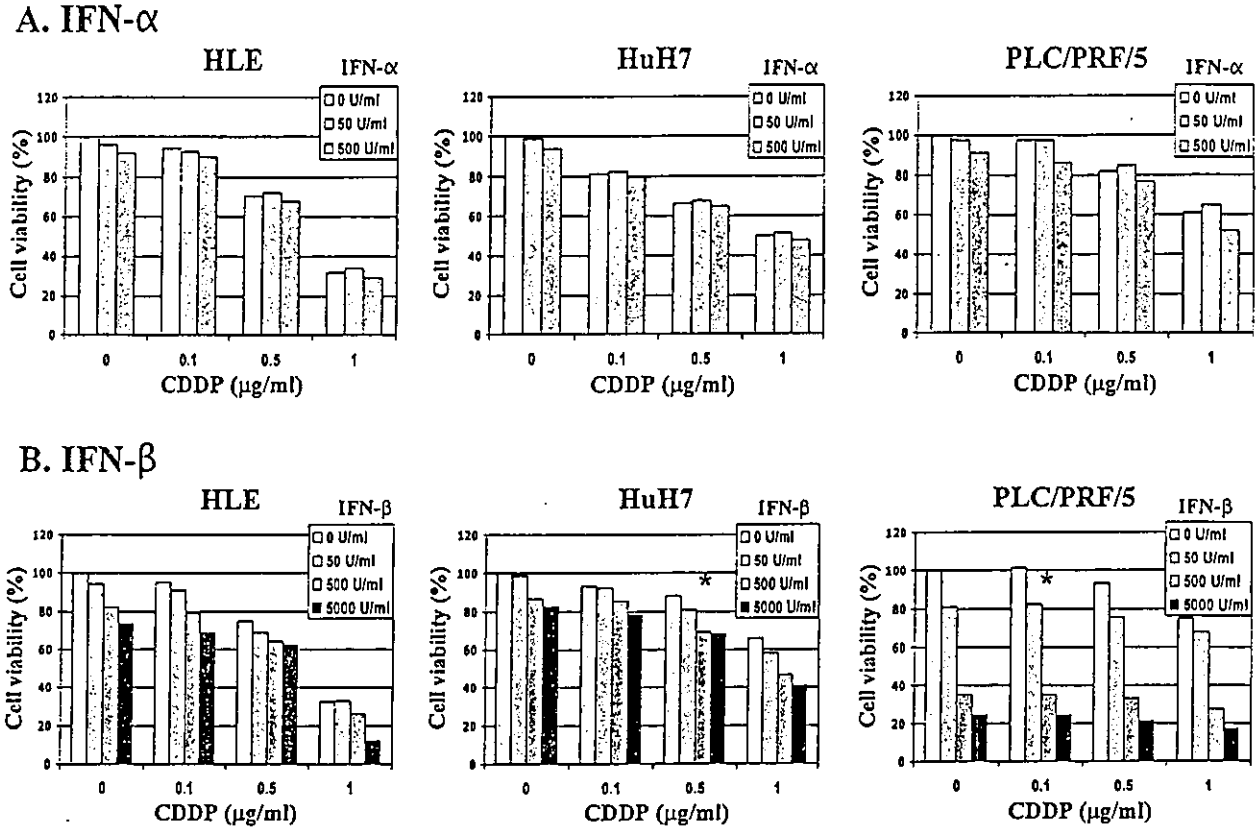


FIG. 3. Growth-inhibitory effects of IFN-α and -β in combination of various doses of cisplatin (CDDP). Cells were incubated with IFN-α (A) or IFN-β (B) in the presence of various concentrations of CDDP and cell proliferation was determined on day 4, as described in Materials and Methods. Proportion of viable cells incubated without drugs was considered 100%. Data are the average of 3 independent experiments. *$P < .05$, denote significant synergistic effect, as examined by isobologram analysis.

stronger than those of IFN-α, and they showed some synergistic effects with 5-FU, CDDP, and DOX.

Both IFN-α and IFN-β belong to the same type of IFNs (type I) and interact with the same IFN-α receptor (IFNAR), but our results showed that their antiproliferative activities were significantly different. IFN-β suppressed the cell proliferation of the cell lines more potently than IFN-α (Fig. 1). Consistent with these results, it has been reported that IFN-β has greater antitumor effects than IFN-α on melanoma, squamous carcinoma, and breast cancer cells.[13–15] One probable mechanism for the different effects may be differences in intracellular signaling, as demonstrated by Shen et al.[16] in rat hepatic stellate cells. Other studies also suggested a tighter interaction of IFN-β than IFN-α to IFNARs and further dimerization of the IFN-β-IFNARs complex.[17,18] In this regard, it is well known that type I IFNs exert their effects through the specific cell surface receptors, IFNARs, which subsequently activate the JAK/STAT pathway.[10] Similar to the differences in their growth-inhibitory effects, previous studies also showed that induction of apoptosis and inhibition of cell cycle by the two IFNs were also different.[19–21] Thus, IFN-β could be a more promising potent agent against human HCC, relative to IFN-α, when combined with anticancer drugs.

The combination chemotherapy with IFN-α has been clinically and experimentally investigated for various cancers.[22] Our study showed that IFN-β, similar to IFN-α, also synergistically inhibited the cell growth of cultured hepatoma cell lines when used with cytotoxic drugs. Among the three agents examined in our study, 5-FU showed the most wide cooperative effect with IFNs (Table 1). One possible mechanism involved in the synergism of 5-FU and IFNs is that the IFNs might increase the amount of active 5-FU metabolites by altering its metabolism or inhibiting over-expression of thymidylate synthase.[23,24] In this regard, we previously demonstrated that IFN-α augments the antitumor effect of 5-FU by inhibiting the progression of the cell cycle, via induction of $p27^{Kip1}$.[25] On the other hand, the biochemical mech-

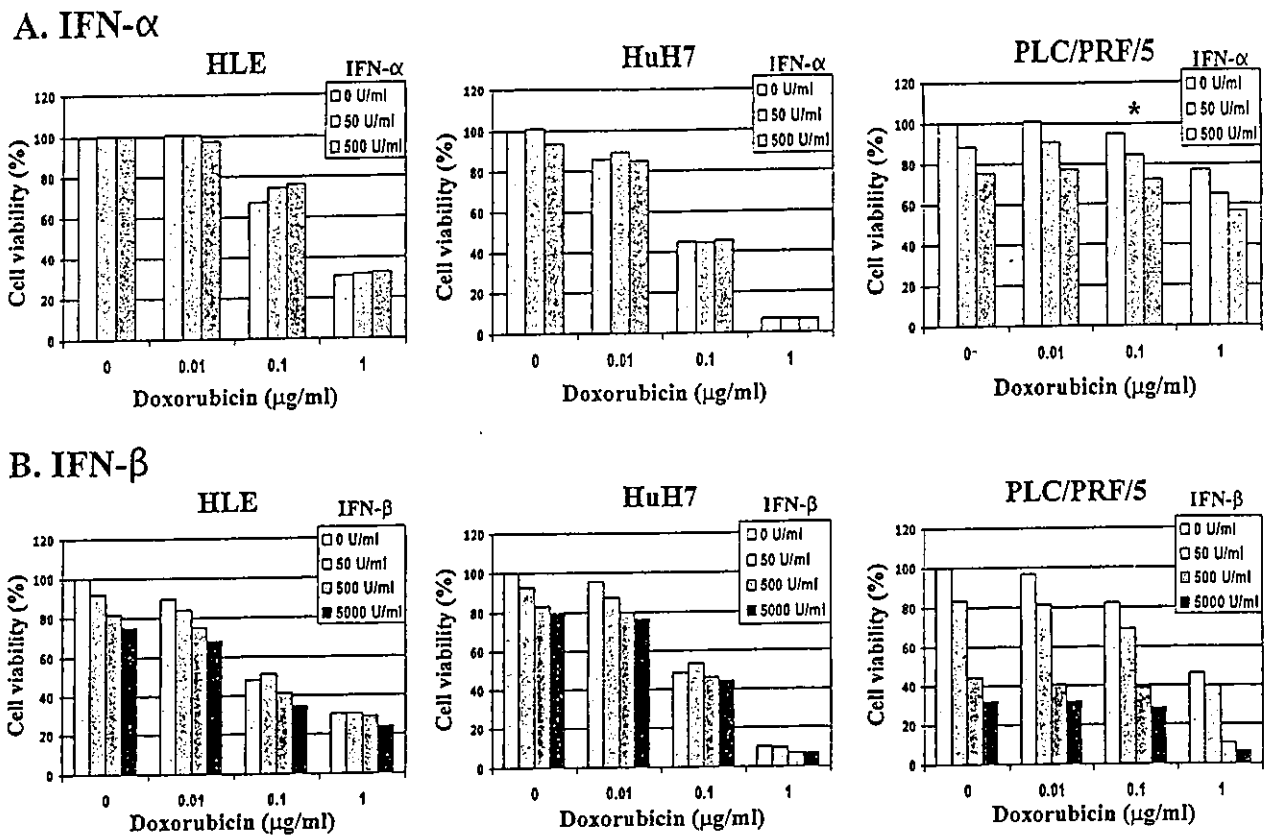


FIG. 4. Growth-inhibitory effects of IFN-α and -β in combination of various doses of doxorubicin. Cells were incubated with IFN-α (A) or IFN-β (B) in the presence of various concentrations of doxorubicin and cell proliferation was determined on day 4, as described in Materials and Methods. Proportion of viable cells incubated without drugs was considered 100%. Data are the average of 3 independent experiments. *$P < .05$, denote significant synergistic effect, as examined by isobologram analysis.

anisms of the synergistic effects of IFNs with CDDP or DOX are poorly understood. However, IFNs are demonstrated to delay the cell cycle mainly in the S phase, which may affect the cellular uptake of anticancer drugs.

Our results showed that PLC/PRF/5 cells were more sensitive to IFN treatment with and without anticancer drugs, compared with the other two cell lines. Interestingly, the expression of IFNAR2 was found in one study to correlate with the growth-inhibitory activity of IFN-α.[25] PLC/PRF/5 cells, which were sensitive to IFN therapy, exhibited high expression of IFNAR2, whereas HuH7 and HLE cells expressed lower levels of the receptor (unpublished results, 2003). We have also reported that IFNAR2 was expressed in primary HCCs, but its level in tissues varied widely.[26] These findings suggest that the expression of IFNAR2 might be an important factor in predicting the effectiveness of IFNs in combination chemotherapies.

TABLE 1. *Cooperative effects of IFN-α and IFN-β in combination with anticancer drugs on three hepatoma cell lines*

| IFN | Anticancer drug | HLE | HuH7 | PLC/PRF/5 |
|---|---|---|---|---|
| −α | 5-FU | Additive/antagonist | Additive/antagonist | Synergistic (.5, 50–500)[a] |
| | CDDP | Additive/antagonist | Additive/antagonist | Additive/antagonist |
| | Doxorubicin | Additive/antagonist | Additive/antagonist | Synergistic (.1, 50) |
| −β | 5-FU | Additive/antagonist | Synergistic (.5, 50–500) | Synergistic (.5, 50) |
| | CDDP | Additive/antagonist | Synergistic (.5, 500) | Synergistic (.1, 500) |
| | Doxorubicin | Additive/antagonist | Additive/antagonist | Additive/antagonist |

IFN, interferon; 5-FU, 5-fluorouracil; CDDP, cisplatin.
[a] Dose of anticancer drug (μg/mL), IFN (IU/mL).